This is to certify that the
thesis entitled

MICROFABRICATION OF AN INTRAOCULAR PRESSURE SENSOR

presented by

YAJUN GU

has been accepted towards fulfillment
of the requirements for the

MASTER OF SCIENCE	degree in	Department of Electrical and Computer Engineering

Major Professor's Signature

Dec. 14, 2005

Date

MICROFABRICATION OF AN INTRAOCULAR PRESSURE SENSOR

By

Yajun Gu

A THESIS

Submitted to
Michigan State University
in partial fulfillment of the requirements
for the degree of

MASTER OF SCIENCE

Department of Electrical and Computer Engineering

2005

ABSTRACT

MICROFABRICATION OF AN INTRAOCULAR PRESSURE SENSOR

By

Yajun Gu

Described in this thesis is the manufacturing for a pressure sensor by utilizing Micro Electrical Mechanical Systems (MEMS) technology. The sensor will be implanted in the eyes of glaucoma patients to monitor intraocular pressure (IOP) on a continuous basis. It is well known that glaucoma is a disease caused by increased IOP resulting either from a malformation or malfunction of the eye's drainage structures. Normal level of IOP is considered to be around 16 mmHg. Pressure over 22 mmHg is considered to moderately high while pressure greater than 45-50 mmHg will be extremely dangerous. This sensor has been designed to measure pressures in the range of 0 to 60 mmHg. We hope that the device will enable doctors to treat their patients better by having a complete patient history of IOP.

The sensor, made of the combination of silicon and Pyrex glass, has an on-chip inductor and a pressure-variable capacitor. That forms an R-L-C resonant circuit. The fabrication of the device involves three steps which are fabrication of the silicon wafer, the Pyrex glass wafer and the assembling step.

ACKNOWLEDGEMENTS

I would like to begin by thanking the Fraunhofer Center for Coatings and Laser Applications for funding this project. I would also like to thank Michael Becker, for his generous help during all the fabrication process. Especially for taking so many nice SEM photos which are necessary for the evaluation of fabrication sequences in this thesis. My deepest gratitude is extended to my committee members, Dr. Jes Asmussen, Dr. Timothy Grotjohn, and Dr. Donnie Reinhard for their valuable input. Finally, I would like to express my utmost appreciation to my advisors, Dr. Jes Asmussen and Dr. Timothy Grotjohn, for their patience and excellent guidance throughout this research.

TABLE OF CONTENTS

LIST OF TABLES

LIST OF FIGURES

Chapter 1

Introduction

1.1 Thesis Statement

Glaucoma is one of the most dangerous diseases of the eye that exists today. It will gradually steal sight without warning and often without symptoms. Vision loss is caused by damage to the optic nerve. This is responsible for carrying the images we see to the brain. High intraocular pressure (IOP) can be associated with much of the development and progression of glaucoma damage that occurs through time. Patients with unilateral elevation of intraocular pressure that is secondary to other eye disorders often develop glaucoma. To monitor the IOP of at risk glaucoma patients in real time, an implantable eye pressure sensor has been designed.

This thesis describes the manufacture and measurement for an implantable eye pressure sensor by using Micro Electrical Mechanical Systems (MEMS) technologies. The sensor will be implanted in the eyes of glaucoma patients to monitor intraocular pressure (IOP) on a continuous basis [1]. This sensor is one of three components in a pressure measurement system. The second component in the system is a data acquisition and processing (DAP) unit. The data from the pressure sensor is received by the DAP unit, which then sends the data to the third component. This third component is a central database that will be utilized for record keeping purposes. Before the pressure sensor will be implanted into human eyes, implantation into cats and primates is planned first.

The work in this thesis is to develop the fabrication procedure of the actual MEMS device based on the design information obtained from a prototype device. All the equipment used in the fabrication process will be introduced. The complete detailed

fabrication "recipe" for this eye pressure sensor is presented, including a flow chart to make every step clearly understood. The rates of various processing steps including boron doping, etching and oxidation, etc. will be determined and the process time will be established. Also device characterization will be done including SEM (scanning electron microscope) pictures to show the cross-section of the device. In the actual fabrication of the devices, many individual devices will be made from a single wafer, and the entire wafer will be fabricated at once. Tens to hundreds of devices will be completed simultaneously.

1.2 Thesis Outline

The main parts of this thesis include the theoretical model of the eye pressure sensor, the component design of silicon wafer and glass wafer, the whole manufacture process and a presentation of experimental measurements and results. In chapter 2, the basic introduction of glaucoma and theoretical background of the entire eye pressure measurement system is presented. The design of the eye pressure sensor and overview of fabrication is presented in chapter 3. Overall size, material selection, and general layout are considered. The component design of silicon wafer and glass wafer is based on the requirements of the pressure sensor's precision. In chapter 4, all the equipment used in fabrication process is introduced. The rates of boron doping, etching and oxidation, etc will be determined in chapter 5. Also the goal of this chapter is to convey an understanding of the methods used to create the samples in this research, so that each step

can be clearly understood and visualized. In chapter 6, the experimental aspect of this research, including the entire detailed manufacturing step is described. Chapter 7 will include all the results we have, such as thickness of the layers, resistivity etc. Conclusions and future works will be presented in Chapter 8.

References:

1. John C. Morrison, Irvin P. Pollack, "Glaucoma: science and practice", New York: Thieme Medical Publishers, c2003.

Chapter 2

Background Information

2.1 What is Glaucoma?

2.1.1 How does Eye Work?

To understand glaucoma, we must first understand how the eye works. Our eye works like a camera. The white part on the outside of the eyeball is called the sclera. In its center is the cornea, the transparent part of the eye that covers the iris or colored part of the eye. The iris operates like a camera shutter by controlling the amount of light that enters the eye. Located behind the iris is the eye lens. It is suspended by fibers that tighten or loosen to focus the light rays from objects outside the eye onto the retina, located at the back of the eye.

The vitreous chamber, made up of clear, gelatinous fluid, is the space between the lens and the retina. The retina is like film in a camera. Within its layers are the cells that perceive light and color. The images received by the retina are conveyed to the brain by the optic nerve, allowing us to see objects. [1]

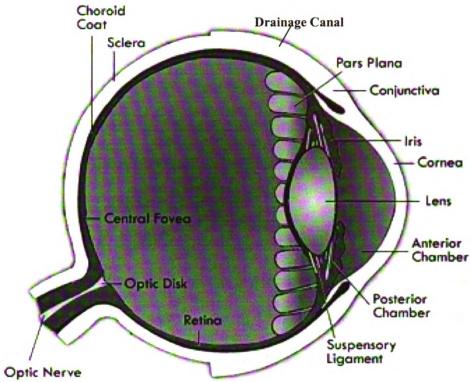

Figure 2.1-How the eye works [1]

2.1.2 What's Glaucoma?

Glaucoma is a group of eye diseases that gradually steals sight without warning and often without symptoms [2]. Vision loss is caused by damage to the optic nerve. This nerve acts like an electric cable with over a million wires and is responsible for carrying the images we see to the brain.

These are several numbers that can explain how important the care about glaucoma should be. [3]

- It is estimated that over 3 million Americans have glaucoma but only half of those know they have it.

- Approximately 120,000 are blind from glaucoma, accounting for 9% to 12% of all cases of blindness in the U.S.
- About 2% of the population ages 40-50 and 8% over 70 have elevated IOP (Intraocular Pressure).
- Glaucoma is the second leading cause of blindness in the U.S. and the first leading cause of preventable blindness.
- Glaucoma is the leading cause of blindness among African-Americans.
- Glaucoma is 6 to 8 times more common in African-Americans than Caucasians.
- African-Americans ages 45-65 are 14 to 17 times more likely to go blind from glaucoma than Caucasians with glaucoma in the same age group.
- The most common form, Open Angle Glaucoma, accounts for 19% of all blindness among African-Americans compared to 6% in Caucasians. [4]
- Other high-risk groups include: people over 60, family members of those already diagnosed, diabetics, and people who are severely nearsighted.
- Estimates put the total number of suspected cases of glaucoma at around 65 million worldwide. [5]

There are two main types of glaucoma which are open angle glaucoma, or primary open angle glaucoma (POAG), and angle closure glaucoma.

- Primary Open Angle Glaucoma

This is the most common form of glaucoma, affecting about three million Americans. It happens when the eye's drainage canals become clogged over time. The intraocular

pressure (IOP) rises because the correct amount of fluid can't drain out of the eye. With open angle glaucoma, the entrances to the drainage canals are clear and should be working correctly. The clogging problem occurs inside the drainage canals (see Figure 2.1). Most people have no symptoms and no early warning signs. If open angle glaucoma is not diagnosed and treated, it can cause a gradual loss of vision. This type of glaucoma develops slowly and sometimes without noticeable sight loss for many years. It usually responds well to medication, especially if caught early and treated.

- Angle Closure Glaucoma

This type of glaucoma is also known as acute glaucoma or narrow angle glaucoma. It is rare and is very different from open angle glaucoma in that the eye pressure usually goes up very fast. This happens when the drainage canals get blocked or covered over, like the clog in a sink when something is covering the drain. With angle closure glaucoma, the iris and cornea is not as wide and open as it should be. The outer edge of the iris bunches up over the drainage canals, when the pupil enlarges too much or too quickly [6].

2.1.3 Effort by Clinicians, Scientists and Engineers

Currently, there is no cure for glaucoma. Glaucoma is a chronic disease that must be treated for life. However, much is happening in research that makes us hopeful a cure

may be realized in our lifetime. There is exciting work being conducted by scientists all over the world in the areas of genetics, neuroprotection and neuroregeneration. These areas of study deal with the origins and pathology of glaucoma as opposed to managing symptoms.

Also work has been done by engineers. Since measuring and monitoring of IOP is crucial, our work of this eye pressure sensor is to make this job easier for the diagnosis, treatment, management and research of glaucoma.

At the present time, regular glaucoma check-ups include two routine eye tests: tonometry and ophthalmoscopy.

- Tonometry

The tonometry test measures the inner pressure of the eye. Usually drops are used to numb the eye. Then the doctor or technician will use a special device that measures the eye's pressure.

Figure 2.2 Tonometry [3]

- Ophthalmoscopy

Ophthalmoscopy is used to examine the inside of the eye, especially the optic nerve. In a darkened room, the doctor will magnify your eye by using an ophthalmoscope (an instrument with a small light on the end). This helps the doctor look at the shape and color of the optic nerve.

Figure 2.3 Ophthalmoscopy [3]

While tonometry is considered to be very accurate for measuring IOP, there are several drawbacks. The oculist can only make a single reading for the particular instant in time that the test is performed. Also the patient is required to visit a oculist's office, thus individual measurements may be separated by long periods of time. Permanent damage to many parts of the eye, including the optic nerve and retina, can result within hours of the onset if the pressures are high enough [3]. If the patients start with the high eye pressures, it is critical that IOP levels be monitored on a continuous basis so that pressure relieving drugs can be administered immediately.

This eye pressure monitoring system will provide benefits not only in clinical applications but also in research of the disease. Clinically, the primary targets for such a device would be patients with severe cases of glaucoma. New York Glaucoma Research Institute's report: "Although IOP is clearly a risk factor, we now know that other factors must also be involved because even people with 'normal' IOP can experience vision loss from glaucoma." It seems oculists still don't know what the large concern is; the peak pressure over twenty four hours, the difference between the high and low pressure measurements for a day, the cumulative IOP over a period of time, or an average IOP level [3]. It is quite possible that one or all of these factors plays a significant role in the progression of glaucoma. In this regard, an IOP sensing device could lead to an extensive gain in research of glaucoma and better methods of treatment.

2.1.4 Implant Options

Basically the eye pressure sensor will be placed inside the eyeball. There are two options for the location of the sensor implant. The device will be located either in the vitreal chamber (option 1 in figure 2.4) or the anterior chamber (option 2 in figure 2.4). The implant will be attached to the wall of the eye or attached to a tether so that the device can easily be located if there is a need for it to be removed.

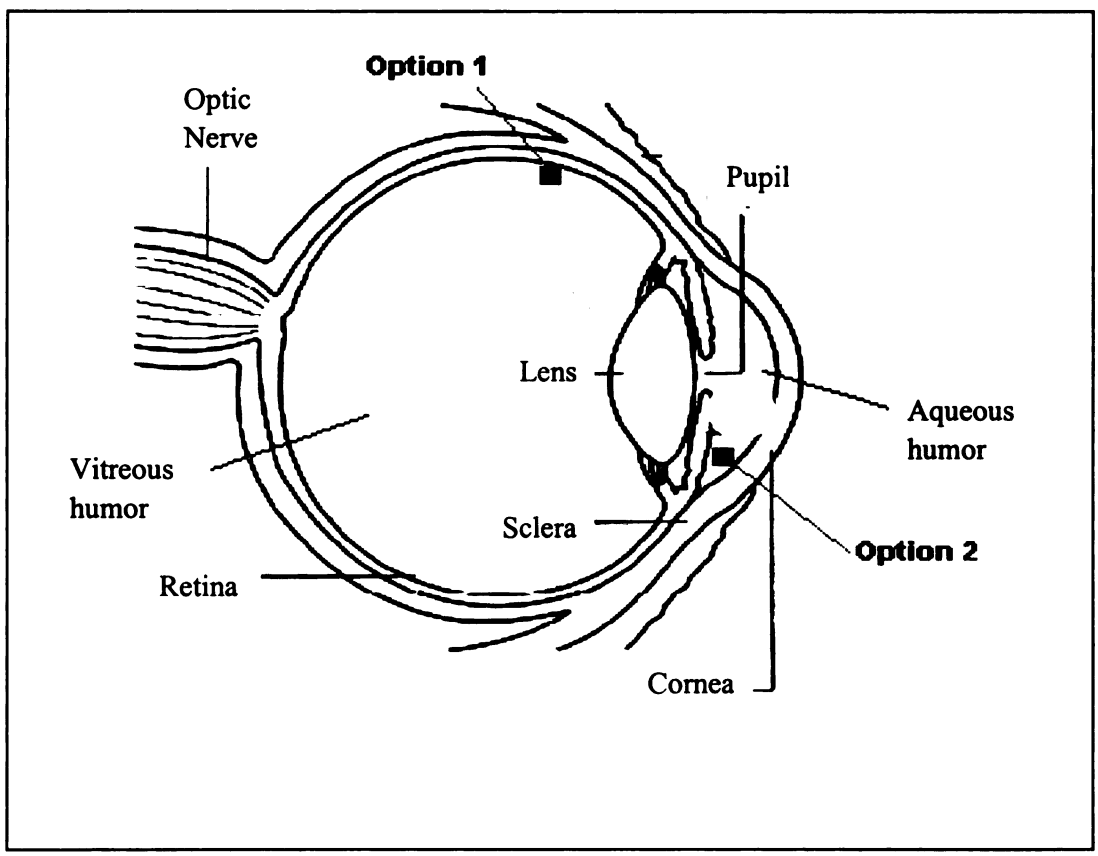

Figure 2.4 Options for Implant Location in the Eye (adapted from [3])

2.1.5 Operation Range

Normal level of IOP is considered to be around 16 mmHg. Pressure over 22 mmHg is considered to be moderately high while pressure greater than 45-50 mmHg is extremely dangerous [3]. This sensor has been designed to measure pressures in the range of 0 to 60 mmHg. It should be noted that all parameters were designed with the intent of manufacturing a device that can accurately produce full-scale measurements up to 60mmHg. However, additional safety factors were included so that the device would remain functional even if the IOP should exceed the 60 mmHg limit of the design.

2.2 Theoretical Model

2.2.1 Overview

The intraocular eye pressure monitoring system consists of three separate components: (Figure 2.5)

1. a wireless, batteryless, remote pressure sensor that is implanted inside the eye of the patient
2. a data acquisition and processing (DAP) unit located external to the body
3. a central data storage system that maintains and compares a time record of the patient's IOP measurements

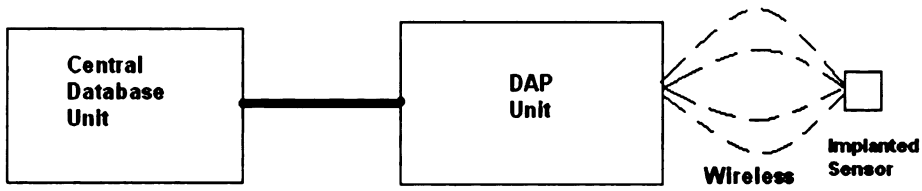

Figure 2.5 Major Structure of Eye Pressure Sensor

We will consider the second component as the primary electrical circuit, while the first component as the secondary electrical circuit. The primary and secondary circuits communicate by means of inductive coupling. The primary circuit generates and transmits a time-wise periodic signal to the secondary circuit, or sensor. The excitation of the sensor feeds back to primary circuit and changes the characteristics of primary circuit which provides information about the electronics, specifically the capacitance of the sensor circuit, which is directly related to the pressure that is being exerted on the sensor.

The base of the eye pressure sensor is a rigid structure which is made of Pyrex glass. There is a flexible diaphragm representing the upper capacitor plate. Around the capacitor plate a planar coil is arranged which is connected to the upper silicon wafer to form an inductor-capacitor circuit. This wafer will be micro-machined and heavily doped with Boron to form a thin P^+ silicon diaphragm. The heavy doping makes the material conductive so the diaphragm can be used as a variable capacitor along with an electrode that is housed on the glass wafer. Finally the Pyrex glass and the silicon substrates are air-tight bonded. With changing outer pressure the diaphragm is arching and the distance

between the capacitor plates is decreasing. This results in a modified capacitance and thus a changed resonant frequency.

2.2.2 Structure of the Circuits

The eye pressure sensor is an inductively coupled device and a schematic of the equivalent R-L-C circuit is shown in Figure 2.6.

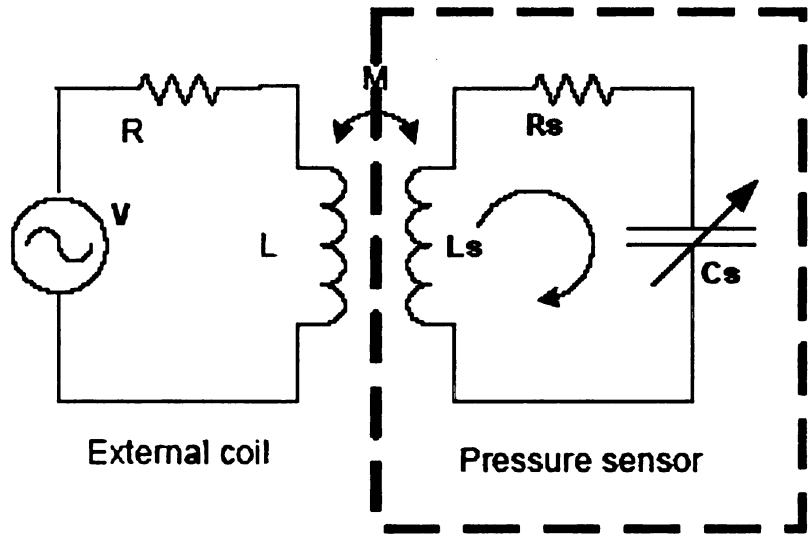

Figure 2.6 Equivalent Circuit

The external circuit (primary circuit) consists of a sinusoidal AC voltage source (V), an inductor (L) and a resistor (R). The eye pressure sensor circuit (secondary circuit) utilizes a pressure sensitive, variable capacitor (C_s) and an inductor (L_s). Any inductor must be wound with a wire that has some resistance, so it is impossible to have an

inductor without some finite resistance. In the equivalent circuit, the resistance in the coil can be considered as a separate resistor (R_s). [7]

2.2.3 Circuit Analysis

The analysis will start from the external circuit. Assume that the voltage generated by the source is a forcing function of the form

$$v(t) = V\cos(\omega t) \tag{2.1}$$

An important expression that relates sinusoids to exponentials is Euler's identity; it states:

$$e^{\pm j\omega t} = \cos(\omega t) \pm j\sin(\omega t) \tag{2.2}$$

$$\mathrm{Re}[e^{j\omega t}] = \cos(\omega t) \tag{2.3}$$

$$\mathrm{Im}[e^{j\omega t}] = \sin(\omega t) \tag{2.4}$$

Thus, the cosine in (2.1) can be expressed as the real part of an exponential with an imaginary exponent:

$$v(t) = \mathrm{Re}[V e^{j\omega t}] \tag{2.5}$$

or more specifically

$$v(t) = \mathrm{Re}[V\cos(\omega t) + jV\sin(\omega t)] \tag{2.6}$$

Equation (2.6) states that the original assumption for v(t) in equation (2.1) can be written as the sum of two functions; one real and one imaginary. The real part of the equation (2.6) is the initial assumed form for v(t) from equation (2.1) with a non-existent imaginary part. However, the complex notation in (2.5) is convenient for the circuit

analysis, so it will be used noting that the imaginary component is non-existent in the solution.

The expected response can also be expressed based on Kirchhoff's Current and Voltage Laws (KCL and KVL respectively). To do this, the current i(t) must also be represented at the same frequency [8] as

$$i(t) = I\cos(\omega t + \phi) = \mathrm{Re}[Ie^{j(\omega t + \phi)}] \qquad (2.7)$$

Every steady state voltage or current in the circuit will have the same form and same frequency ω as a result of KVL. We can write another expression for the voltage:

$$v(t) = \mathrm{Re}[V\angle\Theta\, e^{j\omega t}] = \mathrm{Re}[V\angle 0^{\circ} e^{j\omega t}] \qquad (2.8)$$

where Θ is the phase angle of the voltage such that Θ=0 for a pure cosine wave.

So the response is:

$$i(t) = \mathrm{Re}[I\angle\phi\, e^{j\omega t}] \qquad (2.9)$$

Noting that the complex numbers ($V\angle 0^{\circ}$ and $I\angle\phi$) represent the voltage and the current in terms of magnitude and phase, we will use complex representation (bold letters) **V** and **I** instead. The voltage and current expressions with phasor notation are $\mathbf{V} = V\angle 0^{\circ}$ and $\mathbf{I} = I\angle\phi$. So equation (2.8) and (2.9) become:

$$v(t) = \mathbf{V}e^{j\omega t} \qquad (2.10)$$

$$i(t) = \mathbf{I}e^{j\omega t} \qquad (2.11)$$

According to Kirchhoff's voltage law (KVL) "The algebraic sum of all voltages encountered in traversing any closed path in a lumped connected circuit is zero at any instant of time." For the primary circuit,

$$Ri(t) + L\frac{di(t)}{dt} = v(t) \qquad (2.12)$$

Substituting equations (2.10) and (2.11) in to equation (2.12) gives

$$\mathbf{R\,I}e^{j\omega t} + L\frac{d}{dt}\,\mathbf{I}e^{j\omega t} = \mathbf{V}e^{j\omega t} \qquad (2.13)$$

Eliminate $e^{j\omega t}$, then we get

$$\mathbf{RI} + j\,\omega\,L\mathbf{I} = \mathbf{V} \qquad (2.14)$$

Impedance, designated by Z, is defined as the ratio of the phasor voltage to the phasor current.

$$Z = \frac{V}{I} = R + j\,\omega\,L \qquad (2.15)$$

and its reciprocal, the admittance, designated by Y, as follow

$$Y = \frac{I}{V} = \frac{1}{Z} \qquad (2.16)$$

In rectangular form, the impedance can be written in a general form as a complex number.

$$Z(\omega) = R(\omega) + jX(\omega) \qquad (2.17)$$

$$Y(\omega) = G(\omega) + jB(\omega) \qquad (2.18)$$

R = real part of Z: resistance component

X = imaginary part of Z: reactance component

G = real part of Y: conductance component

B = imaginary part of Y: susceptance component

Each individual element has associated impedance.

For the inductor:

$$Z_L = j\,\omega\,L \qquad X_L = \omega\,L \qquad (2.19)$$

$$Y_L = -j\frac{1}{\omega L} \qquad B_L = -\frac{1}{\omega L} \qquad (2.20)$$

For the capacitor:

$$Z_C = -j\frac{1}{\omega C} \qquad X_C = -\frac{1}{\omega C} \tag{2.21}$$

$$Y_C = j\,\omega\,C \qquad B_C = \omega\,C \tag{2.22}$$

When the external coil (primary circuit) and pressure sensor (secondary circuit) are placed close together, a current in the primary circuit may give rise to a flux through the secondary circuit; hence a changing current in one may cause an induced electrical magnetic field in the secondary circuit. Expressing this quantitatively, a current **I** in the primary circuit causes a flux:

$$N = MI \tag{2.23}$$

through the secondary circuit. When **I** changes, there is induced in the secondary circuit an e.m.f.:

$$V_s = -\frac{dN}{dt} = -M\frac{dI}{dt} \tag{2.24}$$

The mutual inductance M is defined either as the flux through the secondary circuit due to unit current in the primary, or as the electrical magnetic function induced in the secondary circuit per unit rate of change of current in the primary. [9]

This mutual inductance serves as the pseudo driving voltage and a current is induced in the secondary circuit. From (2.15) we recall that the total impedance is equal to the sum of the impedances of the individual elements of the circuit. An expression for the total impedance of the secondary circuit (Z_s) driven by the mutual inductance can be derived.

$$Z_s(\omega) = R_s(\omega) + jX_{Ls}(\omega) + jX_{Cs}(\omega) \tag{2.25}$$

We can use equation (2.19) and (2.21) to replace $X_{Ls}(\omega)$ and $X_{Cs}(\omega)$

$$Z_s(\omega) = R_s(\omega) + j\,\omega\,L_s - \frac{j}{\omega Cs} \tag{2.26}$$

So let's draw another figure 2.7 to show the impedance of the primary and secondary circuits based on the preceding circuit analysis.

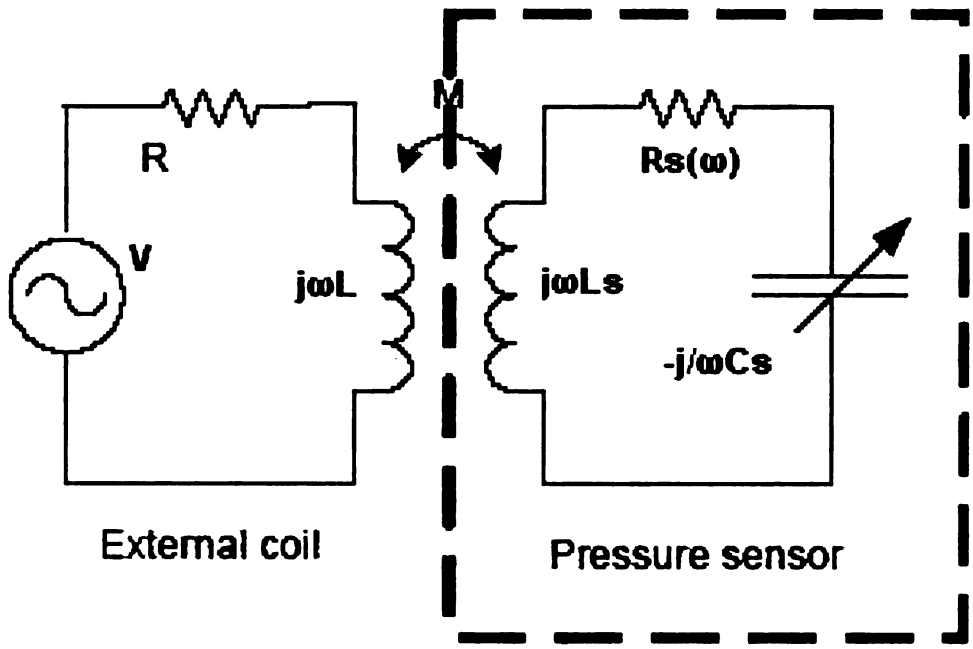

Figure 2.7 Impedances of Individual Elements

According to equation (2.26), the total impedance of the secondary circuit is a function of frequency. The capacitive and inductive impedances will cancel out at a certain frequency so the impedance at that frequency will be purely resistive. At low frequencies, the capacitive reactance predominates and X is negative. At high frequencies, the inductive reactance predominates and X is positive. Since the two reactances vary in opposite ways with frequency, there will be some frequency at which the two are equal and of opposite sign. At that frequency the two reactances will cancel, making X = 0. There, the impedance, and hence also the admittance, is purely real. The voltage and current at the terminals will be in phase. This frequency is called the resonant frequency

and corresponds to the maximum excitation of the secondary circuit. [9]

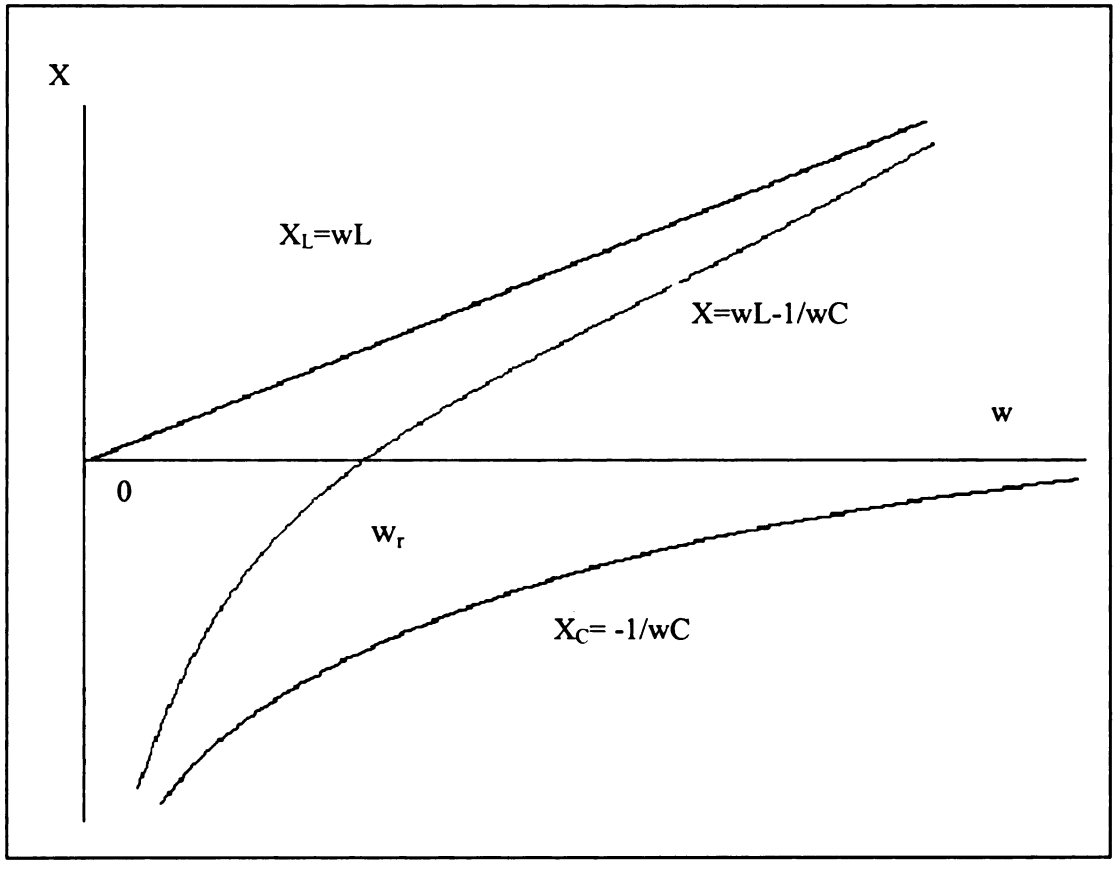

Figure 2.8 Reactance Curve

For the inductive impedance and capacitive impedance to cancel, we must have

$$j\,\omega\,L_s = j/\,\omega\,C_s \tag{2.27}$$

Algebraically reorganizing leads to

$$\omega_r^2 = 1/L_sC_s \Rightarrow \omega_r = 1/\sqrt{LsCs} \tag{2.28}$$

measured in units of radians per second.

It is more convenient to use the following form

$$f_r = \frac{1}{2\pi\sqrt{LsCs}} \tag{2.29}$$

measured in units of hertz.

As a result of the inductive and capacitive impedances canceling at the resonant frequency, the total impedance is due to the resistance only. At resonance, a local minimum in the secondary circuit's impedance occurs. This local minimum in the impedance corresponds to a maximum degree of excitation for the secondary circuit.

We next write KVL around the external circuit and pressure sensor circuit loops. Figure 2.9 is the equivalent circuit including impedance from mutual inductance.

$$jX_M(\omega) = \frac{(\omega M)^2}{Zs(\omega)} \qquad (2.30)$$

$$Z(\omega) = \frac{V}{I} = R + j\omega L + jX_M(\omega) \qquad (2.31)$$

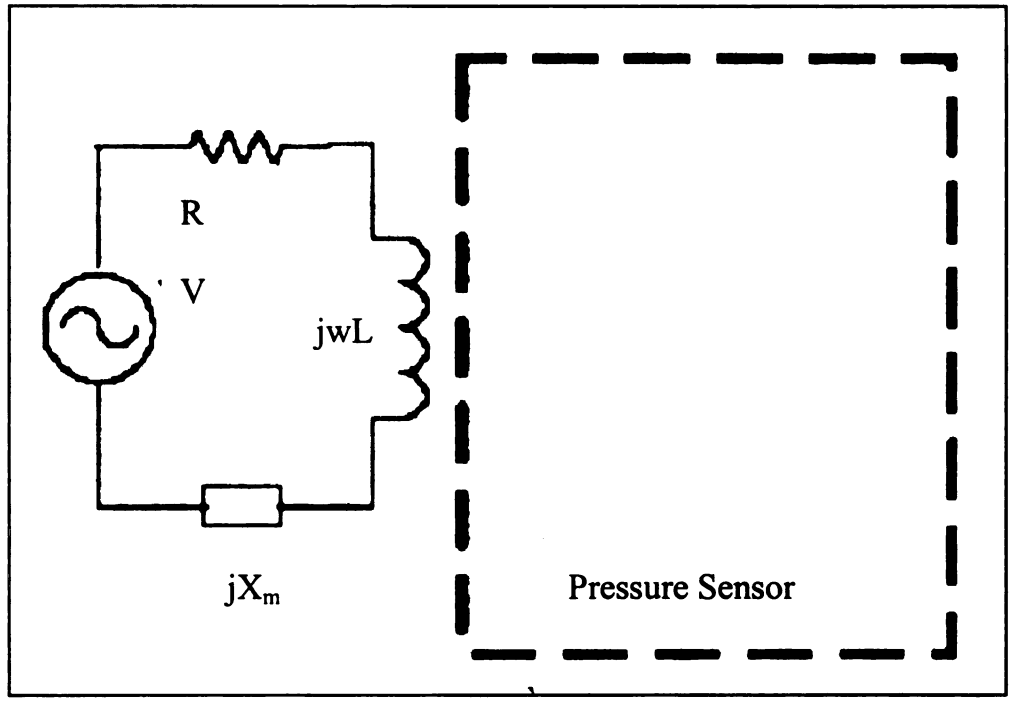

Figure 2.9 Equivalent Circuit Including Impedance from Mutual Inductance

After substituting in the impedance of the secondary circuit, the expression for reactance due to the mutual inductance becomes

$$jX_M(\omega) = \frac{(\omega M)^2}{Rs(\omega) + j\omega Ls - \frac{j}{\omega Cs}} \qquad (2.32)$$

$X_M(\omega)$ is inversely proportional to the impedance of the secondary circuit (Z_s). As stated previously, the impedance of the secondary circuit is at a local minimum at the resonant frequency since the inductive and capacitive reactance cancel. As a result, $X_M(\omega)$ will have a local maximum value which is dependant on $R_s(\omega)$ only. Now we can rewrite (2.31) as

$$Z(\omega) = \frac{V}{I} = R + j\omega L + \frac{(\omega M)^2}{Rs(\omega) + j\omega Ls - \frac{j}{\omega Cs}} \qquad (2.33)$$

Since the combined impedance due to the inductor and the mutual inductance ($j\omega L + jX_M(\omega)$) shows a local maximum at the resonant frequency, the voltage drop due to these elements is also at the maximum [11]. Due to equation (2.33), the magnitude of the voltage drop across the load resistor V_r will dip (as shown on Figure 2.10).

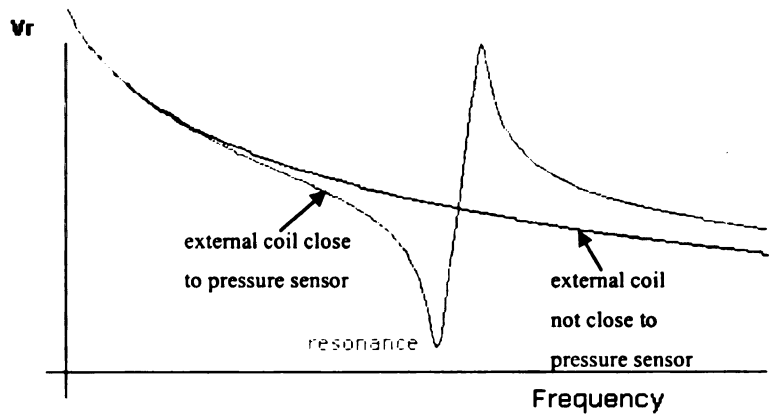

Figure 2.10 Voltage dip due to the resonance

In order to detect the resonant frequency, a periodic signal will be swept through a

particular frequency range and the voltage across the load resistor will be measured to find the resonant frequency by finding the frequency at which the minimum occurs.

The effect of the resistance of the secondary circuit is to increase the frequency range that is required for the peak to occur after voltage dip. As the resistance increases, the voltage dip will occur prior to the resonant frequency, and the rise will occur after the resonant frequency. With a resistance of 50 Ohms in the secondary circuit, for example, the frequency range will be about 5 MHz, with the dip occurring about 2 MHz prior to the resonant frequency and the peak of the rise occurring about 3 MHz after the resonant frequency [11].

Once the resonant frequency has been determined, equation (2.29) can be used to determine the capacitance. Since the inductance is a known, fixed value, the only variable in the equation is capacitance. The capacitance, in turn, is dependant on the pressure on the membrane only.

References:

1. Myron Yanoff, Jay S. Duker, James J. Augsburger ... [et al.] "Ophthalmology", St. Louis, MO : Mosby, c2004.

2. John C. Morrison, Irvin P. Pollack, "Glaucoma: science and practice", New York : Thieme Medical Publishers, c2003.

3. New York Glaucoma Research Institute, http://www.glaucoma.org/

4. Baltimore.N, "Racial differences in the cause-specific prevalence of blindness in east", Engl J Med. 1991 Nov 14;325(20):1412-7;

5. Quigley, "Number of people with glaucoma worldwide", 1996, http://www.glaucoma.org/

6. Douglas Rhee, "Glaucoma", New York : McGraw-Hill, Medical Pub. Division, c2003.

7. The Bureau of Naval Personnel, "Basic Electricity", Dover Publications. New York. 1969

8. Norman Balabanian, "Electric Circuits", McGraw-Hill, Inc. New York. 1994

9. W. M. Gibson, "Basic Electricity", Longman, London and New York, 1969

10. Karl F. kuhn, "Basic Physics", J. Wiley, New York, c1996

11. Gregory Alan Goodall, "Design of an implantable micro-scale pressure sensor for managing glaucoma", Michigan State University, Department of Mechanical Engineering; 2002

Chapter 3

Sensor Design and Fabrication Overview

3.1 Design Parameters

3.1.1 Overall Size

The design of the eye pressure sensor is presented in this chapter. Based on the use of the eye pressure sensor, there are only two places that the sensor can be placed in the eye. One option is in the vitreal chamber and the other option is in the anterior chamber (Figure 2.4). So the overall size of the sensor must be very small to allow a trouble-free implantation. The ophthalmologists associated with this project have constrained the largest dimension to not exceed about 3 millimeters [1]. Anything larger than this could result in interference with normal vision or complicate the implantation process. Since the overall size of the pressure sensor must be less than 3 millimeter, this constraint is the most important parameter and will take precedence over all of the other factors in the design. The best way to produce a working sensor in this size range is to use micro fabrication techniques. Once it has been insured that the size constraint has been satisfied, maximizing the sensitivity of the device is the next concern.

3.1.2 Material Selection

Since the eye pressure sensor will be implanted inside the eyeball, it is very important that the sensor be made of biocompatible materials. And according to the overall size (not exceeding about 3 millimeters), the best suitable material is silicon and

glass because most MEMS sensors utilize silicon and glass, which should be biocompatible (still under testing). Silicon is utilized because so much is known about it, and fabrication processes used to manufacture silicon devices are much more developed than for other materials [2]. Glass is readily available and is very compatible with many fabrication processes. Pyrex glass, one type of the glass, has a compatible thermal expansion with silicon. It will be easy for us to use them to do the bonding process. For these reasons, silicon and glass are chosen as the materials for all of the external structures.

3.1.3 General Layout

A general sensor design is shown below.

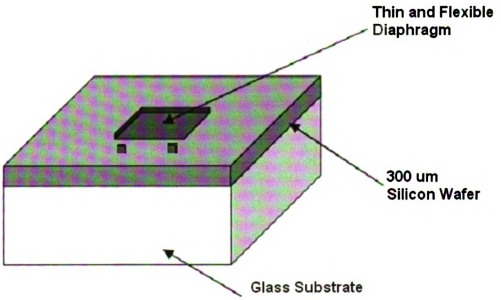

Figure 3.1 General Layout of this eye pressure sensor

The base of the eye pressure sensor is a rigid structure which is made of Pyrex glass. The flexible diaphragm represents the upper capacitor plate, while the second capacitor plate facing the diaphragm is located on top of the glass substrate. Around the capacitor plate a planar coil is arranged which is connected to the upper silicon wafer. The top wafer will be made of (100) silicon. This wafer will be micro-machined and heavily doped with boron to form a thin P^+ silicon diaphragm. The heavy doping makes the material conductive so the diaphragm can be used as a variable capacitor along with the electrode that is housed on the glass wafer. Also the heavily doped silicon can be used to stop the etching process.

Finally the Pyrex glass and the silicon substrates are bonded together air-tight (the bonding process will be introduced in the manufacturing chapter). With changing outer pressure the diaphragm is arching and the distance between the capacitor plates is decreasing. This results in a modified capacity and thus a changed resonant frequency.

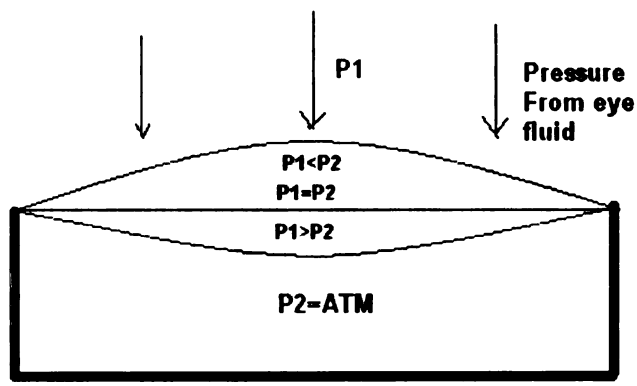

Figure 3.2 Diaphragm under Pressure

3.2 Silicon Component Design

The device will be a box with width and length of around 3000 microns depending on how to cut into its final shape. The silicon wafer to be used is 300 microns thick. The Pyrex glass wafers to be used for the substrate are typically available with a standard thickness of 500 microns. So the total thickness of the device is around 800 microns.

The silicon wafer houses the upper capacitor plate. As mentioned before this plate operates as a flexible diaphragm. The diaphragm will have a thickness of 4 microns [1]. The bottom of the silicon wafer will be etched so that a 1.5 micron deep recess is created to define the capacitive gap. The final dimensions of the upper sensor plate results from calculations of the silicon deflection for a certain thickness and area and the distance between the two plates. A cross section with the most important dimensions of the final silicon structure is shown in the picture below. (Figure 3.3)

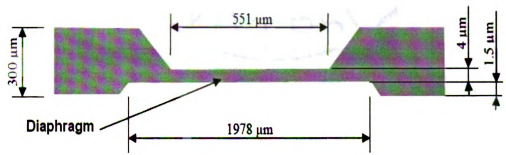

Figure 3.3 Dimensions of Diaphragm Structure Created from Silicon Wafer

3.3 Glass Component Design

The glass assembly houses the lower capacitor plate and the inductor. The inductor will consist of 23 turns of gold wire. The wire will be electroplated on to the glass substrate. Gold was selected as the wire and plate material because of its good conductive properties and the workability at small structures. The physical dimensions are shown in Figure 3.4. The inside dimension of the coil will be 530 microns with 12-micron gaps between each turn. The wire will have a line width of 17 microns.

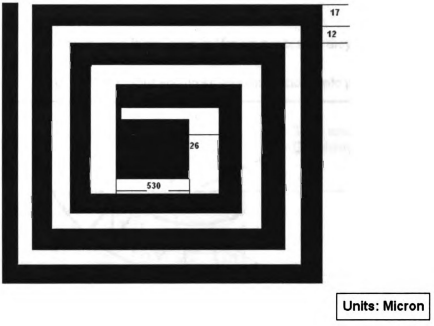

Figure 3.4 Portion of the Inductor Layout

The figure 3.5 shows in the cross section of the glass wafer.

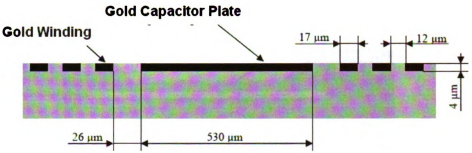

Figure 3.5 Pyrex Wafer Cross Section

3.4 Assemble

Once the silicon wafer and Pyrex glass wafer are processed they will be bonded together. Below is the overall blueprint and cross section of the whole pressure sensor.

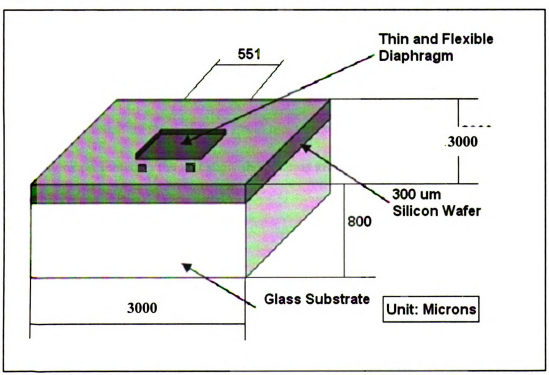

Figure 3.6 Dimension of the silicon wafer and glass wafer

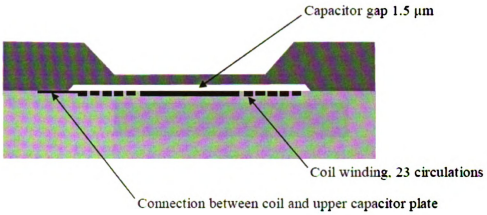

Figure 3.7 Cross section of the pressure sensor [3]

3.5 Fabrication Overview

In this section, the fabrication process is overviewed. There are 14 fabrication steps for the silicon wafer, 12 steps for the Pyrex glass wafer, and 4 steps for the assembling. An inspection by microscope or Scanning Electrical Microscope (SEM) is required after finishing most of the steps to make sure the pattern or trench is intact. The illustrations presented in the text show the patterns after every step.

3.5.1 Silicon Wafer Part

There are 14 fabrication steps for the silicon wafer. A silicon dioxide layer will be used as the mask. A silicon etch will be performed to form a cavity to house the upper

capacitor plate. Boron doping layer is used as the etch stop. Back side etching will be done after bonding to form a 4 micron thick membrane.

1) Substrate cleaning

2) Thermal oxidation of the wafer

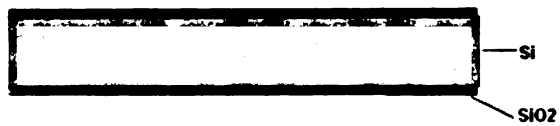

3) Photoresist spinning on both sides and lithographic step

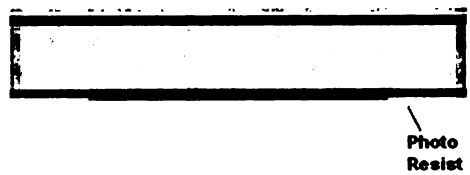

4) SiO2 etching

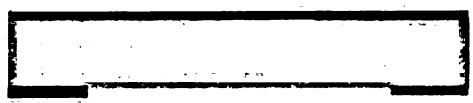

5) Photoresist removal

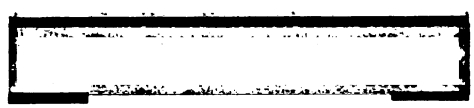

6) Slow Silicon etching to form cavity

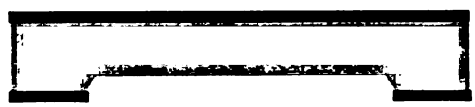

7) Photoresist spinning

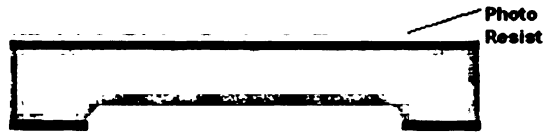

8) SiO_2 removal

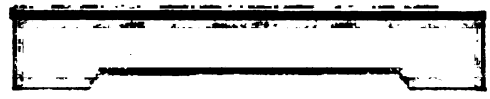

9) Photoresist removal and cleaning

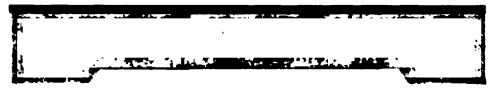

10) Boron Nitride (BN) wafer activation (Optional)

11) Boron doping

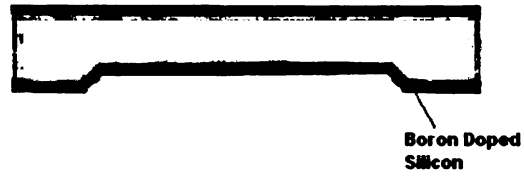

12) Photoresist spinning and lithographic step on top side

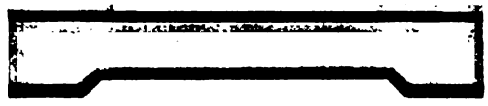

13) SiO_2 etching

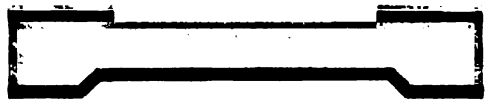

14) Photoresist removal and cleaning

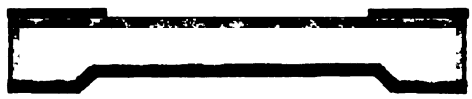

3.5.2 Glass Wafer Part

There are 12 fabrication steps for the Pyrex glass wafer. An aluminum layer is used as the mask. Pyrex glass etch will be performed to form 23 gold wire windings.

1) Substrate cleaning

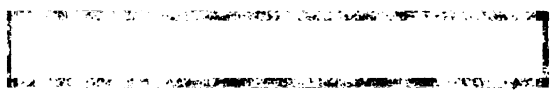

2) Aluminum deposition

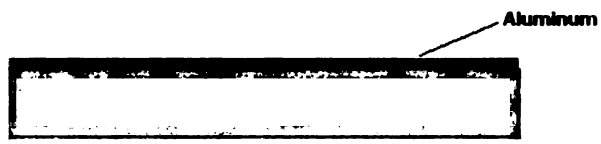

3) Lithography step: defining coil, capacitor plate and electrical contacts

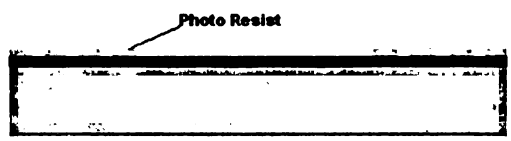

4) Aluminum etching

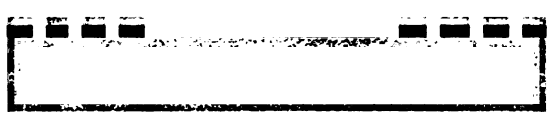

5) Pyrex glass etching (with depth of 2 microns)

6) Photoresist removal

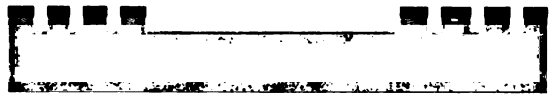

7) Aluminum removal

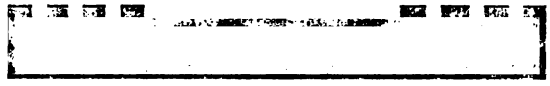

8) PVD process to coat Titanium and Gold seed layer

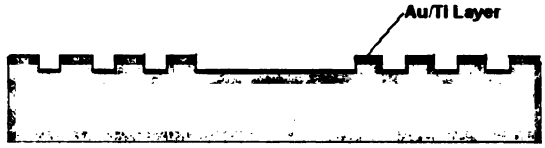

9) Lithography step (including mask alignment)

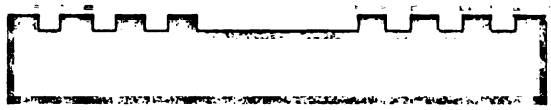

10) Electroplating: deposition of 4 μm gold

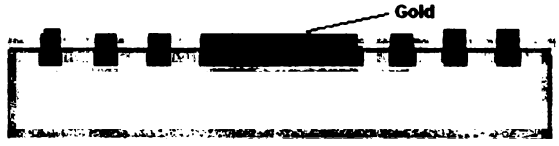

11) Removal of Photoresist with acetone

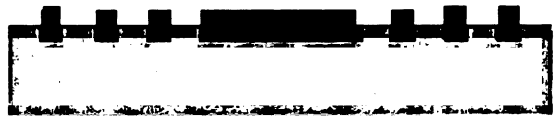

12) Thin Au/Ti layer removal

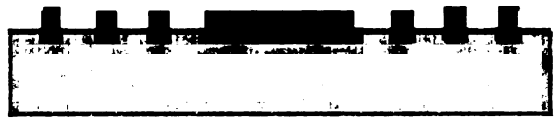

3.5.3 Assembling Part

There are 4 fabrication steps for assembling the part. The Pyrex glass and the silicon substrates are bonded together air-tight. Back etch is performed to form a 4 micron thick membrane.

1) Cleaning procedure (Piranha)

2) Anodic bonding

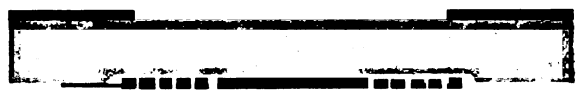

3) Back silicon etching

4) Separation

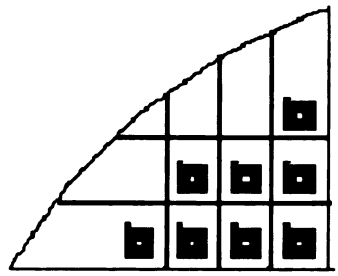

References:

1. Gregory Alan Goodall, "Design of an implantable micro-scale pressure sensor for managing glaucoma", Michigan State University, Department of Mechanical Engineering; 2002

2. K. Najafi, "Lecture Notes from EECS 498 at the University of Michigan", Fall semester lecture 10, P.21, Fall, 2001

3. Kevin Krieger, "Internship report of Manufacturing of an eye pressure sensor", 2003

Chapter 4

Experimental Equipment and Method

4.1 Introduction

In this chapter, we will discuss the equipment used in the fabrication process to achieve the design of the eye pressure sensor. The normal operating procedure of the equipment will be presented. Also the techniques used to characterize the device are introduced.

4.2 Substrate Cleaning

4.2.1 Initial Wafer Clean

An acetone ultrasonic bath and a methanol ultrasonic bath are used as the degreaser of the substrates and isopropanol is used to relieve water from the substrate. Figure 4.1 shows two ultrasonic baths we use in this experiment.

Figure 4.1 Acetone Ultrasonic Bath

Acetone is a colorless, volatile, aliphatic, extremely flammable liquid ketone, CH_3COCH_3, widely used in industry as a solvent for numerous organic substances. If the wafer has obvious dirt or fingerprints, when we put it with acetone into the ultrasonic bath, the organic substances will be easily removed.

Methanol is a colorless, toxic, flammable liquid, CH_3OH, used as antifreeze, a general solvent, a fuel, and a denaturant for ethyl alcohol. Methanol is a monohydric alcohol. It is used as a solvent for varnishes and grease. In our cleaning procedure, methanol is used as a general solvent after acetone, since it also removes the acetone residue.

Isopropanol is a clear, flammable liquid, $(CH_3)_2CHOH$, that is miscible with water. Isopropanol is a secondary alcohol. It is one of the cheapest alcohols and has replaced ethanol for many uses because of its similar solvent properties. We use its

property that it is easily miscible with water in order to remove the water from the substrate [1].

De-ionized (DI) water is used as an essential ingredient in the manufacturing procedure. The vast majority of dissolved impurities in modern water supplies are ions such as calcium, sodium, chlorides, etc. The deionization process removes ions from water via ion exchange. Figure 4.2 shows SUPER-Q De-ionized water system in our clean room.

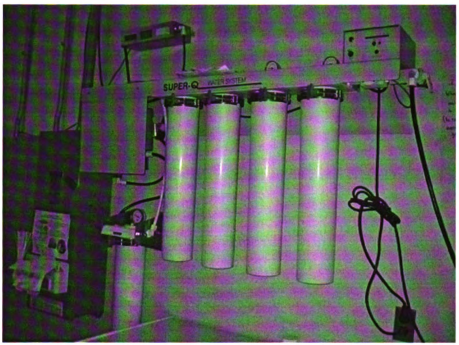

Figure 4.2 SUPER-Q De-ionized water system

4.2.2 RCA Wafer Clean

The RCA clean is the industry standard for removing contaminants from wafers. Werner Kern developed the basic procedure in 1965 while working for RCA (Radio

Corporation of America) - hence the name [2]. Over time many companies have tried to improve the effectiveness through variations in the original recipe. The solution 10:2:1 of (H_2O:H_2O_2:NH_4OH) has been used here as it is especially good for the removal of grease and other organics from wafer.

4.2.3 Piranha Wafer Clean

Piranha is a cleaning solution consisting of a H_2SO_4:H_2O_2 mixture typically in 3: 1 ratio. It produces a strongly oxidizing clean and is used to remove organic materials, including remaining photoresist from the wafer surface. It is typically applied first in the cleaning sequence.

4.3 Thermal Oxidation

4.3.1 Introduction

The oxide of silicon, or silicon dioxide (SiO_2), is one of the most important ingredients in semiconductor manufacturing, having played a crucial role in the development of semiconductor planar processing. During the fabrication process of the eye pressure sensor, the SiO_2 layer is used to mask the silicon for the etching process. Silicon is etched in our procedure with KOH. The SiO_2 etch rate with KOH as the

etchant is very small as compared to the silicon etch rate. Thus SiO_2 is a suitable mask material.

The formation of SiO_2 on a silicon surface is most often accomplished through a process called thermal oxidation. Thermal oxidation, as its name implies, is a technique that uses extremely high temperatures (usually between 700-1300°C) to accelerate the growth rate of oxide layers.

The thermal oxidation of SiO_2 consists of exposing the silicon substrate to an oxidizing environment of O_2 or H_2O at elevated temperature, producing oxide films whose thicknesses range from 60 to 20000 angstroms. Oxidation of silicon is not difficult, since silicon has a natural inclination to form a stable oxide even at room temperature, as long as an oxidizing ambient is present. The elevated temperature used in thermal oxidation therefore serves primarily as an accelerator of the oxidation process, resulting in thicker oxide layers per unit of time.

4.3.2 Oxidation Furnace

Thermal oxidation is accomplished using our oxidation furnace, which provides the heat needed to elevate the oxidizing ambient temperature. The oxidation furnace typically consists of:

1) A cabinet;

2) A heating system;

3) A temperature measurement and control system;

4) A fused quartz process tube where the wafers undergo oxidation;

5) A system for moving process gases into and out of the process tubes;

6) A loading station used for loading (or unloading) wafers into (or from) the process tubes.

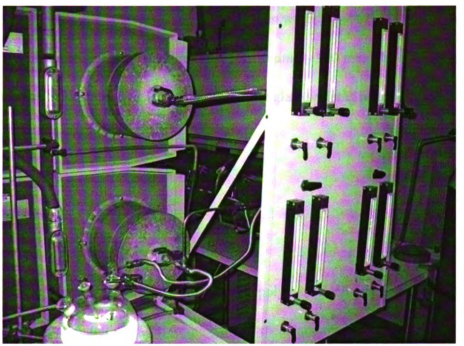

Figure 4.3 Oxidation Furnace

The heating system consists of several heating coils that control the temperature around the furnace tubes. The wafers are placed in quartz glassware known as boats. A boat can contain up to 50 wafers. The oxidizing agent (oxygen or steam) then enters the process tube through its source end, subsequently diffuses to the wafers where the oxidation occurs.

4.4 Lithography Step

4.4.1 Introduction

Lithography is a very important step of MEMS applications, as it is one of the best methods currently in use for manufacturing devices on scales with micrometer dimensions. In our procedure, one side of the silicon wafer is patterned with an array of squares, each square measuring approximately 930 μm by 940 μm. The other side is also patterned with squares as 2 mm by 2 mm. The glass wafer is patterned with 23 turns of recess for the coil.

4.4.2 Photoresist

Photoresist is a polyimide photosensitive polymer which comes in liquid form. The liquid is spun onto the wafer, forming a thin sheet, and then cured in an oven to form a resistant plastic coating. Photoresist is classified into two groups, positive resists, in which the exposed areas become more sensitive to chemical etching and are removed in the developing process, and negative resists, in which the exposed areas become resistant to chemical etching, so the unexposed areas are removed during the developing process [1].

We use Shipley 1813 as our positive photoresist. The spin program is set to spin 30 seconds at 3000 rpm with a ramp rate of about 1000 rpm/sec. The resulting wafer should have a uniform coating of photoresist on its surface, approximately 1.3 μm (this is what 1813 stands for).

HMDS (Hexamethyldisilazane) is an optional step. It is an adhesion promoter and will help the photoresist stick to the wafer. In general, if the wafer is clean and dry, the HMDS is probably not needed.

4.4.3 Spinner

A full feature spinner from Laurell Technologies Corporation is used in our experiment. The spinner has been machined from solid virgin grade materials which do not degrade or generate particles. The bowl-shaped interior forces fluid downward where it is routed directly to the rear drain. The upper plenum closes inside the base providing an overlapping seal. It's programmable, so 30 seconds 3000 rpm spin with a ramp rate of 1000 rpm/sec is set up for our experiment. Figure 4.4 shows the spinner.

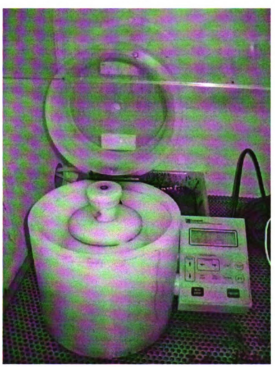

Figure 4.4 Spinner

4.4.4 Masks Design

Making masks for optical printing starts with square glass plates. The plates are first coated with a material opaque in the wavelength region used to expose resist [3]. Chromium is used in our masks. Then we draw the pattern with AutoCAD tools and print it onto the glass plates. Figure 4.5 is the design of coils with dimensions. There are 23 windings for each coil and 245 coils in a 3-inch wafer. The inside diameter of the coil will be 520 microns. The designed inductance of the device is then 0.3 μH. All masks are made by Photo Sciences Inc.

coil with dimensions (µm)

23 windings, canal width
10, ligament width 19

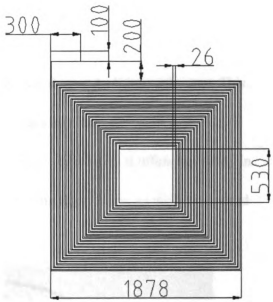

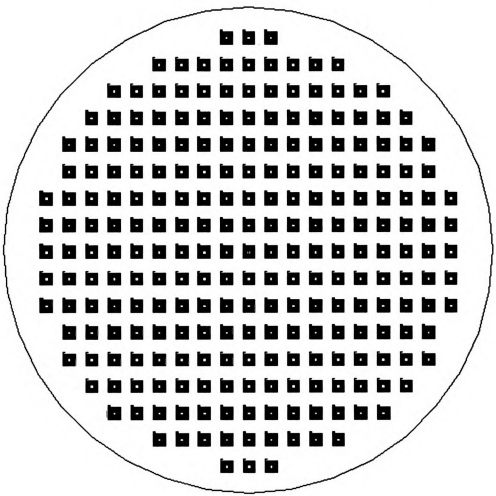

Figure 4.5 Design of Mask

4.4.5 Mask Aligner

An MJB 3 mask aligner from Karl Suss is used during the lithography step. This machine is widely used for MEMS and optoelectronics applications. It is a high resolution manual mask aligner capable to print features of 0.5 μm. It offers flexibility in the handling of irregularly shaped substrates of differing thicknesses, as well as standard size wafer up to 3 inches diameter.

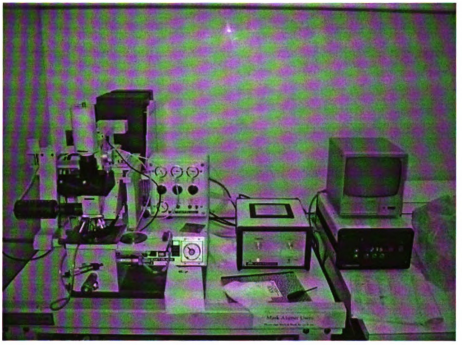

Figure 4.6 SUSS MJB3 Mask Aligner

4.5 PVD Coating

Physical vapor deposition methods are clean, dry vacuum deposition methods in which the coating is deposited over the entire object simultaneously, rather than in

localized areas. The technique consists of evaporating material in a hard vacuum (typically < 10^{-5} torr) and allowing it to hit the substrate in the chamber.

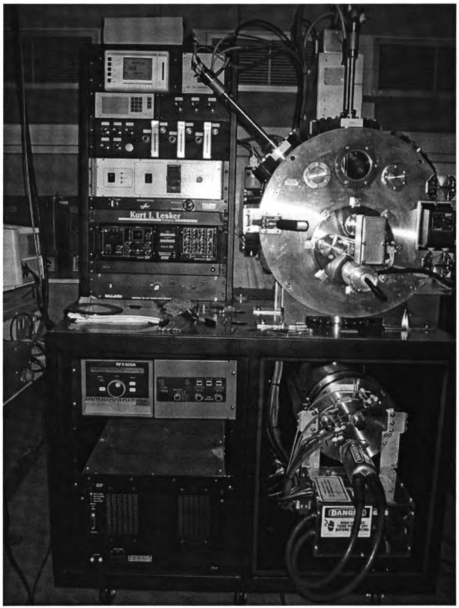

Figure 4.7 Physical Vapor Deposition System From Kurt J. Lesker Inc.

The PVD system shown in Figure 4.7 is used to deposit a Ti/Au layer on a glass surface at low temperature. However, a thickness of 4 microns cannot be realized with PVD due to the resulting layer stress. That is why we deposit a thin gold layer first and

increase the gold layer thickness by electroplating. The gold adhesion on glass is not very good. Thus, a seed layer, for example titanium, with a better adhesion is used.

For our purpose an e-beam PVD system is used. This system is able to evaporate different metallic materials. First, titanium and gold are put in crucibles. It's important to not overfill the crucible so that it doesn't overflow when the e-beam melts the material. Next, the glass wafer is installed facing the crucible. Afterwards, the system was pumped down to high vacuum. A high vacuum of about $5*10^{-6}$ Torr is necessary to avoid collisions between the e-beam electrons and gas atoms. After this, the e-beam was directed to the middle of the crucible and the e-beam current was adjusted in a way that the coating material starts to vaporize. The deposition rate and current layer thickness is shown by the deposition monitor which works via the piezo-crystal oscillator principle. The rate is generally controlled to be less than 1.0 Angstrom/sec. The deposition time is approximately 35 minutes for the 200nm aluminum layer, 10 minutes for the 50nm gold seed layer and 5 minutes for the 5nm Titanium layer.

4.6 Anodic Bonding

4.6.1 Introduction

The glass type selected for the eye pressure sensor is Pyrex because of the similar thermal expansion between Pyrex and silicon. Anodic bonding, also referred to as field assisted glass-silicon sealing, is a process of bonding a silicon wafer to glass under the

influence of high temperature and an externally applied electric field. In order for good contact to occur, the two surfaces to be bonded must be quite smooth with roughness less than 0.1 μm [4]. In a typical anodic bonding procedure, the wafers to be bonded are assembled together and heated on a hotplate to about 500°C with a bias of 1000V.

4.6.2 Generic Anodic Bonding Setup

Figure 4.8 gives a schematic drawing of a generic anodic bonding setup. A D.C. power supply connected to the assembly such that the positive terminal is connected to the silicon wafer and the negative terminal is connected to the Pyrex glass wafer. When an electric field of several hundred to a thousand volts is applied across the assembly, the glass seals to the silicon wafer. The bonded areas initially appear as dark regions starting in the area where the voltage is directly applied. Eventually these splotches cover the entire surface. The resulting bond is essentially irreversible. Figure 4.9 shows the actual equipment used for the anodic bonding process.

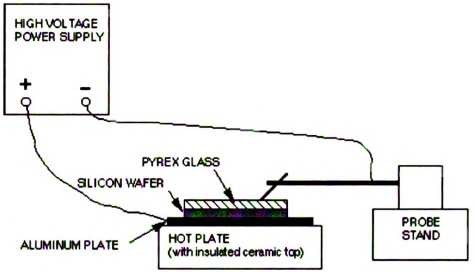

Figure 4.8 Generic Anodic Bonding Setup

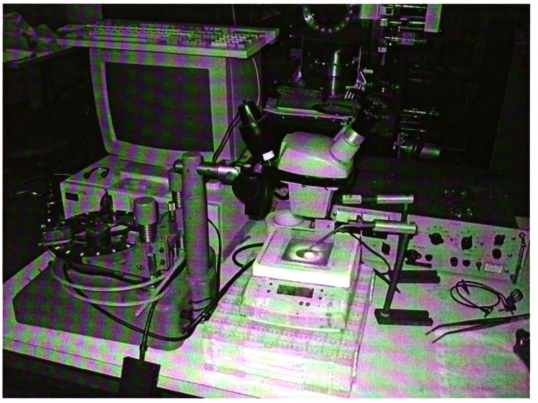

Figure 4.9 Anodic Bonding Equipment

The bonding mechanism itself is due to the presence of mobile sodium ions in the Pyrex glass. At an elevated temperature the positive sodium ions in the glass have an

increased mobility and are attracted to the negative electrode on the glass surface. This leaves behind negatively charged oxygen ions adjacent to the silicon surface. Initially the potential is uniformly distributed across the glass, but with the increased temperature and voltage, a large potential drop develops between the Pyrex glass and the anode. The resulting electric field between the surfaces pulls them into intimate contact, possibly creating covalent bonds. Figure 4.10 illustrates this process.

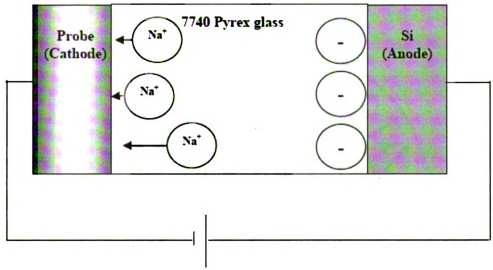

Figure 4.10 The Anodic Bonding Process between Silicon and Pyrex 7740 glass

4.7 Separating/Dicing

Once the silicon wafer and Pyrex wafer are bonded, it needs to be diced into individual devices. One 3 inch diameter wafer combination houses 243 sensors. For cutting a SXJ-2 precision wire saw is used. It is designed to provide a very smooth cutting for all kinds of materials, especially for very fragile crystals and substrates such as Silicon, GaAs etc. It is equipped with a sample holder to hold samples of any shape.

SXJ-2 wire saw's stage can rotate 360 degree horizontally and 30 degree vertically. It has wire blade tension adjustable device to provide accurate cuttings.

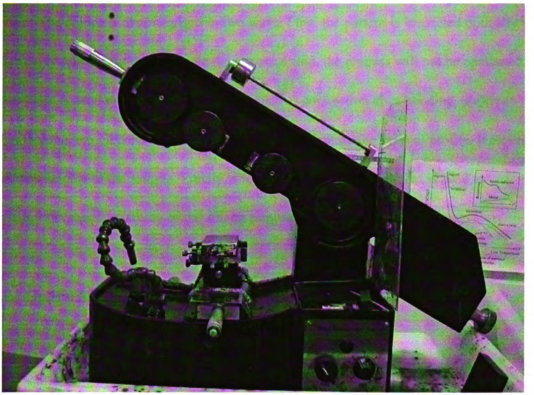

Figure 4.11 SXJ-2 Precision Wire Saw

The wafer dicing works using the following method. An aluminum substrate with a little wax on top is heated up on a heat plate. When the wax is melting, the wafer is pushed into the soft wax. After the wax cooled down, it is solidified and binds the wafer to the substrate. The wire saw has a holding device to fix the aluminum substrate and thus the wafer in the right cutting position. The cutting width is approximately 0.5 mm for the wire saw.

4.8 Device Characterization

4.8.1 Introduction

The device is characterized in two ways. First, the pattern is inspected optically after every fabrication step. If some defects are found, the process will not be continued. Also SEM is used to check selected details such as connection after bonding, undercut after etching, etc. Second, a profilometer is used to measure the vertical profile. It records the step-heights of the sample. Finally, a four point probe measurement is used to measure the sheet resistivity of the silicon sample after boron doping.

4.8.2 Optical Microscope

A CX RII microscope from Microscoptics Inc. which has a 1000 x maximum magnification is used for pattern assessment. It has internal ruler to measure the size of the pattern without taking any pictures. Also the microscope comes with a ZEISS MC63A Video Capture system. That permits high resolution pictures to be taken.

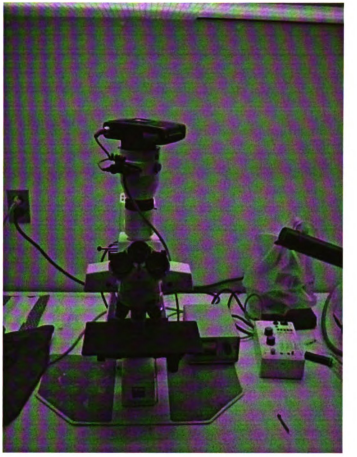

Figure 4.12 CX RII microscope from Microscoptics Inc.

4.8.3 Scanning Electron Microscopy (SEM)

At certain points in this experiment, SEM images were used to evaluate fabrication sequences. An Electron Optics Laboratories 6400 SEM was used. This particular SEM is equipped with a lanthanum hexaboride (LaB6) electron source, and has a maximum magnification of 300,000. Such high magnifications are not necessary for evaluation of the features found in our experiment. Different images can be taken with

the SEM including Secondary Electron Imaging, Backscattered Electron Imaging, and Energy Dispersive X-ray Microanalysis (EDS).

The SEM requires that the sample be mounted on either a 1-inch diameter or 0.25-inch diameter aluminum stub for insertion into the SEM. This means that the 3-inch wafers we use need to be cut into small pieces to examine them with the SEM. Typically, non-conductive samples must be gold coated for SEM imaging, although it was observed that for moderate accelerating voltages of around 20kV or less, the samples did not need to be coated to produce acceptable images, but that coating made images somewhat easier to obtain.

4.8.4 Profilometer

The Dektak 6M is an thin and thick film step height measurement tool capable of measuring steps with resolution below 100 Å. This tool is used to profile surface topography, as well as measuring surface roughness in the sub-nanometer range. Since the patterns on silicon wafer and Pyrex glass wafer are in the micron range, it's easy for us to trace the profile of the samples and find tiny defects with the Dektak 6M.

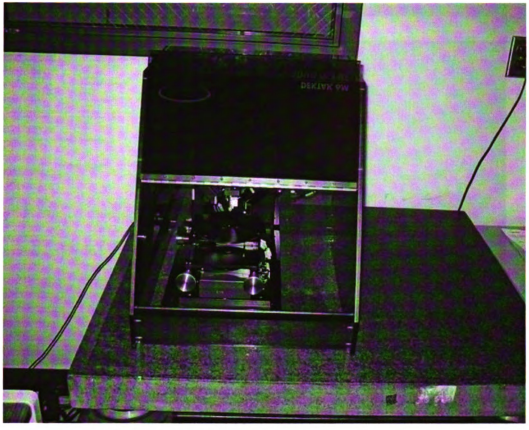

Figure 4.13 Dektak 6M Profilometer

Figure 4.13 shows us the Dektak 6M. Automated step-detection software is available that can provide multi-step detection and that can automatically measure and calculate negative and positive step transitions. The surface roughness can also be calculated. The program as shown in Fig 4.14 is for a glass sample after the electroplating step.

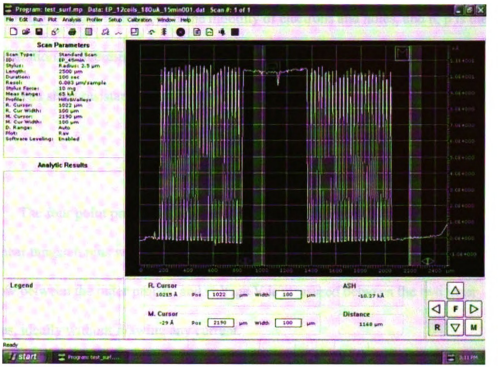

Figure 4.14 Profile of a glass sample after electroplating step for 12 coils-180μA-15minutes.

4.8.5 Four Point Probe Method

A four point probe is used to measure the sheet resistivity of the silicon sample after boron doping.

To understand the four point probe use consider a bar of silicon with length L, width W, and thickness t. The resistance is given by:

$$R = \frac{\rho L}{Wt} \qquad [4.1]$$

where ρ is the resistivity.

If L, W and t are know and R is measured, then the resistivity can be determined. The resistivity is related to the conductivity as $\rho = 1/\sigma$, where the conductivity σ =

$q(\mu_n n + \mu_p p) \sim q\mu_n n$. Here μ_n, μ_p is the mobility of electrons and holes, and n, p is the concentration of electrons and holes. q is the electron charge ($q=1.6*10^{-19}C$).

The sheet resistance is defined as:

$$R_s = \rho/t \qquad [4.2]$$

$$R = R_s(\frac{L}{W}) \qquad [4.3]$$

The four point probe, as depicted schematically in Figure 4.15, contains four thin collinear tungsten pins which are made to contact the sample under test. Current I is made to flow between the outer probes, and voltage V is measured between the two inner probes, ideally without drawing any current.

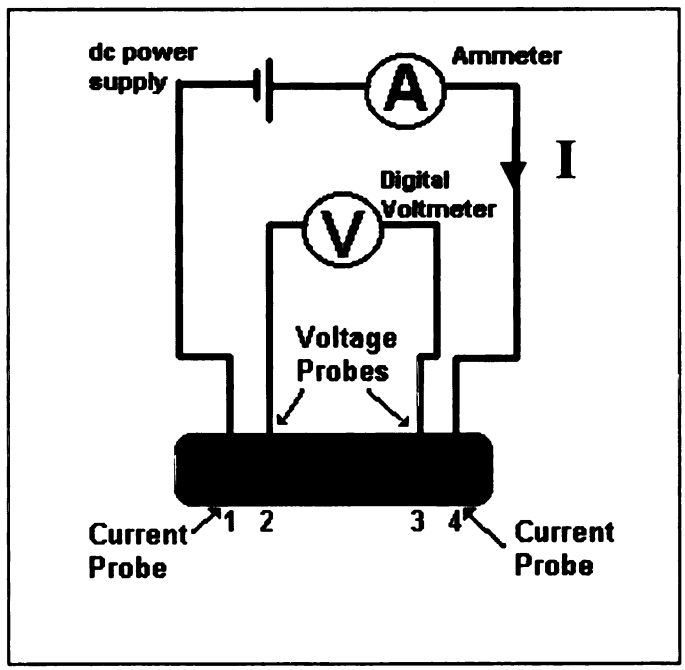

Figure 4.15 Schematic of Four Point Probe

The potential V at a distance r from an electrode carrying a current I in a material of resistivity ρ is

$$V = \frac{\rho I}{2\pi r} \qquad [4.4]$$

For four probes resting on a semi-infinite medium with current entering probe 1 and leaving probe 4,

$$V_2 = \frac{\rho I}{2\pi}\left(\frac{1}{S_{12}} - \frac{1}{S_{23}+S_{34}}\right) \qquad [4.5]$$

$$V_3 = \frac{\rho I}{2\pi}\left(\frac{1}{S_{12}+S_{23}} - \frac{1}{S_{34}}\right) \qquad [4.6]$$

Here S_{12} is the distance between point 1 and 2. (See Figure 4.15)

If $S_{12} = S_{23} = S_{34} = S$

$$V_{23} = \frac{\rho I}{2\pi S} \qquad [4.7]$$

So

$$\rho = 2\pi S\left(\frac{V_{23}}{I}\right) \qquad [4.8]$$

Correction factors are used for real wafers: [2]

1) Finite thickness: Correction factor = $\frac{t/S}{2\ln(2)}$

$$R_s = \frac{\rho}{t} = 4.53\left(\frac{V}{I}\right) \qquad [4.9]$$

2) Finite diameter

$$R_s = \xi\left(\frac{V}{I}\right) \qquad [4.10]$$

ξ is tabulated below as a function of d/S

C.F.$_1$(d/S)	Circle	Square	Rectangle L/W=2	Rectangle L/W=3	Rectangle L/W=4
1.0				0.9988	0.9994
1.25				1.2467	1.2248
1.5			1.4788	1.4893	1.4893
1.75			1.7196	1.7238	1.7238
2.0			1.9475	1.9475	1.9475
2.5			2.3532	2.3541	2.3541
3.0	2.2662	2.4575	2.7000	2.7005	2.7005
4.0	2.9289	3.1127	3.2246	3.2248	3.2248
5.0	3.3625	3.5098	3.5749	3.5750	3.5750
7.5	3.9273	4.0095	4.0361	4.0362	4.0362
10.0	4.1716	4.2209	4.2357	4.2357	4.2357
15.0	4.3646	4.3882	4.3947	4.3947	4.3947
20.0	4.4364	4.4516	4.4553	4.4553	4.4553
32.0	4.4791	4.4878	4.4899	4.4899	4.4899
40.0	4.5076	4.5120	4.5129	4.5129	4.5129
infinity	4.5324	4.5324	4.5325	4.5325	4.5324

Table 4.1 ξ as a function of d/S

For example, if we measure the sheet resistivity of a 3 inch wafer, wafer diameter d=7.62cm, probe distance S=0.102cm, d/S = 75. For d/S > 40, use ξ = 4.53. Figure 4.16 shows the setup of the 4-point probe device used in this study.

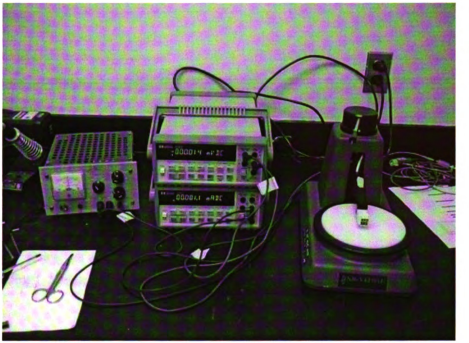

Figure 4.16 Four Point Probe Setup

References:

1. "Merriam-Webster collegiate dictionary", Springfield, Mass: Merriam-Webster, Inc., 2003

2. W. Kern and D. A. Puotinen, "Cleaning Solutions Based on Hydrogen Peroxide for use in Silicon Semiconductor Technology", RCA Review, 187-206, June, 1970

3. W. R. Runyan and K. E. Bean, "Semiconductor Integrated Circuit Processing Technology", Addison-Wesley Publishing Company, 1990

4. J Wei, H Xie, M L Nai, C K Wang, and L C Lee, "Low temperature wafer anodic bonding", Singapore Institute of Manufacturing Technology, Aug. 2002

Chapter 5

Process Specification and Determination of Rates

5.1 Introduction

In this chapter, the process specification and how the rates of each procedure to achieve the design of the eye pressure sensor are presented. Rates of dry oxidation and wet oxidation are needed to form an appropriate mask layer. There are several rates in the etching steps such as silicon dioxide etching, silicon etching, gold etching, etc. Boron doping is a high temperature process that diffuses boron atoms into the silicon wafer. One of the important tasks for the boron doping layer is the use of the doped region as an etch stop to realize the diaphragm thickness of 4 μm. Also the rates of electroplating will be determined in this chapter.

5.2 Rates Determination of Thermal Oxidation

Depending on which oxidant species is used (O_2 or H_2O); the thermal oxidation of silicon may either be in the form of dry oxidation (wherein the oxidant is O_2) or wet oxidation (wherein the oxidant is H_2O). The reactions for dry and wet oxidation are governed by the following equations:

1) dry oxidation: $Si\ (solid) + O_2\ (vapor) \rightarrow SiO_2\ (solid)$ [5.1]

2) wet oxidation: $Si + 2H_2O\ (vapor) \rightarrow SiO_2 + 2H_2\ (vapor)$ [5.2]

During dry oxidation, the silicon wafer reacts with the ambient oxygen, forming a layer of silicon dioxide on its surface. In wet oxidation, water enters the reactor where it

diffuses toward the wafers. The water molecules react with the silicon to produce the oxide and the byproduct hydrogen gas.

These oxidation reactions occur at the Si-SiO_2 interface, i.e., silicon at the interface is consumed as oxidation takes place. As the oxide layer grows, the Si-SiO_2 interface moves into the silicon substrate. As a result, the Si-SiO_2 interface is always below the original Si wafer surface. The SiO_2 surface, on the other hand, is always above the original Si surface. SiO_2 formation therefore proceeds in two directions relative to the original wafer surface.

The amount of silicon consumed by the formation of silicon dioxide is also fairly predictable from the relative densities and molecular weights of Si and SiO_2, i.e., the thickness of silicon consumed is 44% of the final thickness of the oxide formed. Thus, an oxide that is 10000 angstroms thick will consume about 4400 angstroms of silicon from the substrate.

For oxidation processes that have very long durations, the rate of oxide formation may be modeled by a simple equation known as the Parabolic Growth Law : $x_o^2 = B\ t$, where x_o is the thickness of the growing oxide, B is the parabolic rate constant, and t is the oxidation time. This shows that the oxide thickness grown is proportional to the square root of the oxidizing time, which means that the oxide growth is hampered as the oxide thickness increases. This is because the oxidizing species has to travel a greater distance to the Si-SiO_2 interface as the oxide layer thickens.

Oxidation processes that have very short durations, on the other hand, may be modeled by another simple equation known as the Linear Growth Law: $x_o = C\ (t + \tau)$,

where x_o is the thickness of the growing oxide, C is the linear rate constant, t is the oxidation time, and τ is the initial time displacement to account for the formation of the initial oxide layer at the start of the oxidation process.

The Linear and Parabolic Growth Laws were developed by Deal and Grove [1], and are collectively known as the Linear Parabolic Model. This oxide growth model has been empirically proven to be accurate over a wide range of temperatures (700-1,200°C), oxide thicknesses (300-30,000 angstroms), and oxidant partial pressures (0.2-25 atmospheres).

Oxide growth rate is affected by oxidation time (see figure 5.1). More specifically, oxide growth is accelerated by an increase in oxidation temperature or oxidation pressure. Other factors that affect thermal oxidation growth rate for SiO_2 include the crystallographic orientation of the wafer; the wafer's doping level; the presence of halogen impurities in the gas phase; the presence of plasma during growth; and the presence of a photon flux during growth.

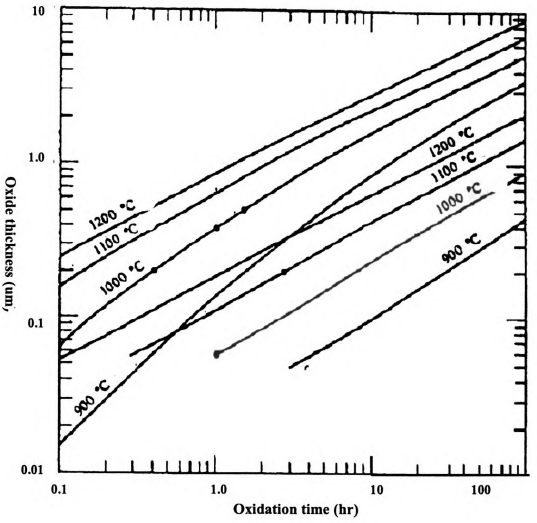

Figure 5.1 Wet and dry silicon dioxide growth rate [1]

5.3 Rates Determination of Etching Step

5.3.1 Introduction

5.3 Rates Determination of Etching Step

5.3.1 Introduction

In some IC manufacturing steps, whole wafers are completely coated with a layer or layers of various materials, such as silicon dioxide, aluminum, titanium, or gold. The unwanted material is then selectively removed by etching through a mask. In addition, various patterns must sometimes be etched directly into the silicon or glass surface. For example, etching the Pyrex glass forms the trench for the gold windings.

Possible kinds of etching are wet chemical, electrochemical, pure plasma etching, reactive ion etching (RIE), ion beam milling, and high-temperature vapor etching [2]. Only wet chemical etching for different kinds of material is used in our process. Wet etching, in which the wafers are immersed in aqueous etching solutions, is the oldest but often still the most inexpensive and efficient process. Etching solution, etching rate, and undercut will be concerned in this section. SEM photographs will be used to compare with different conditions.

5.3.2 Silicon Dioxide Etching

Silicon Dioxide is used as a mask in the fabrication procedure. SiO_2 etching is operated in Silicon-Wafer process steps 4), 8), 13) (see chapter 3). The solution used to

etch SiO_2 is one part 49% HF and five parts 40% NH_4F (Buffered HF, BHF) at room temperature. The etch rate depends on the acid concentration and temperature. The general chemical equation is:

$$SiO_2 + 4HF \rightarrow 2H_2O + SiF_4\,(\text{gaseous}) \qquad [5.3]$$

According to Kirt R. Williams' research, BHF etches the thermal oxide at an approximate rate of 100 nm per minute at 20°C [3], so the etching time of 13 minutes was expected for the 1.3 μm oxide layer used in this study. Our experiments show 10-minute etching is enough for removing the SiO_2 layer, because the clean room's temperature usually is above 20°C.

Since SiO_2 is hydrophilic and silicon is not, the progress of the etch can be monitored by periodically removing the wafer from the etching solution, submerging it in a beaker of water, and then removing the wafer and watching the behavior of the wafer as it streams off the wafer. When the oxide has been removed, the water will run off of the silicon rapidly and essentially completely, while when the wafer is still coated with oxide the water will 'sheet' and cling to the wafer. The oxide etch was terminated when the water test indicated that the SiO_2 had been removed [4].

The goal of the etching step is to transfer the pattern in the photoresist to the oxide. During each etching step, we need to consider the effect of the chemical solution on other existing materials. In this case, BHF etches the Silicon (100) wafer and Shipley 1813 Photoresist at a rate of 0 nm per minute at 20°C [3]. But during our experiment, the photoresist was found to not last more than 10 minutes at 27°C, which is the clean room's temperature.

5.3.3 Silicon Etching

Generally, we differentiate between two etch methods, dry etching (plasma etching) and wet etching (chemical etching). We performed wet etching for silicon. KOH is a commonly used silicon etch chemistry for micromachining silicon wafers. [5] The patterned oxide is used as a mask, because the etch rate of the silicon dioxide layer in the KOH is very small (7.7 nm/min) compared to the etch rate of silicon (around 1100 nm/min). [3] For the deep back etch, we use a highly boron doped region as an etch stop. Highly boron doped region also has a very slow etch rate in KOH.

The general chemical reaction for etching silicon is:

$$Si + 2OH^- + 2H_2O \rightarrow SiO_2(OH)_2^{2-} + 2H_2 \qquad [5.4]$$

Silicon has a face centered cubic structure and is specified by {100}, {110}, and {111} planes. For our process, the best suitable wafer type is the {100} wafer. This means the polished surface of the wafer is a {100} plane.

The wet etching is further segmented into isotropic and anisotropic etching. For the back etch anisotropic wet etching process is required. The KOH etch rate is strongly effected by the crystallographic orientation of the silicon. Table 5.1 relates silicon orientation-dependent etch rates (μm/min) of KOH to crystal orientation with an etching temperature of 70°C. Table 5.1 is taken directly from [6]. In parentheses are normalized values relative to (110).

Crystallographic Orientation	Rates at different KOH Concentration		
	30%	40%	50%
(100)	0.797 (0.548)	0.599 (0.463)	0.539 (0.619)
(110)	1.455 (1.000)	1.294 (1.000)	0.870 (1.000)
(210)	1.561 (1.072)	1.233 (0.953)	0.959 (1.103)
(211)	1.319 (0.906)	0.950 (0.734)	0.621 (0.714)
(221)	0.714 (0.491)	0.544 (0.420)	0.322 (0.371)
(310)	1.456 (1.000)	1.088 (0.841)	0.757 (0.871)
(311)	1.436 (0.987)	1.067 (0.824)	0.746 (0.858)
(320)	1.543 (1.060)	1.287 (0.995)	1.013 (1.165)
(331)	1.160 (0.797)	0.800 (0.619)	0.489 (0.563)
(530)	1.556 (1.069)	1.280 (0.989)	1.033 (1.188)
(540)	1.512 (1.039)	1.287 (0.994)	0.914 (1.051)
(111)	0.005 (0.004)	0.009 (0.007)	0.009 (0.010)

Table 5.1 Anisotropic KOH etching rates vs. orientation

The ideal (110) and (100) surface has a more corrugated atomic structure than the (111) primary surfaces. The (111) plane is an extremely slow etching plane that is tightly packed, has a single dangling-bond per atom, and is overall atomically flat. As shown above, the strongly stepped and vicinal surfaces to the primary planes are typically fast etching surfaces. The etched cavity is thus surrounded by (111) planes only.

Furthermore, KOH etching rates depend on the solution composition and temperature as shown as Table 5.2. As with all wet chemical etching solutions, the dissolution rate is a strong function of temperature. Significantly faster etch rates at higher temperatures are typical, but less ideal etch behavior is also common with more aggressive etch rates [7], [8], [9].

Etchant	Temperature (°C)	Direction (plane)	Etch rate (μm/min)	Remarks	Reference
20% KOH: 80% H_2O	20 40 60 80 100	(100) (100) (100) (100) (100)	0.025 0.188 0.45 1.4 4.1	Near Peak etch rate at the conc. across temperature	[7]
30% KOH: 70% H_2O	20 40 60 80 100 20 40 60 80 100	(100) (100) (100) (100) (100) (110) (110) (110) (110) (110)	0.024 0.108 0.41 1.3 3.8 0.035 0.16 0.62 2.0 5.8	Smoother surfaces than at lower concentration Faster etch rate for (110) than for (100)	[8]
40% KOH: 60% H_2O	20 40 60 80 100	(100) (100) (100) (100) (100)	0.020 0.088 0.33 1.1 3.1		[8]
44% KOH: 56% H_2O	120	(100) (110) (111)	5.8 11.7 0.02	High Temperature	[9]

Table 5.2 KOH etching rates vs. composition and temperature

5.3.4 Pyrex Glass Etching

The original design for the glass wafer is using soda lime glass. It is because that the etch rate depends on the glass type. Pure SiO_2 glass also called quartz glass is very

hard to etch and thus has a small etch rate. Soda lime is not very hard to etch. It consists of 73% SiO_2, 15% Na_2O, and 12% CaO. The etch rate is 10 times higher as compared to quartz glass.

Unfortunately, we found out that soda lime can not be used for our glass wafer because of the difference of the thermal expansion between soda lime and silicon. The soda lime glass was extensively cracked after bonding (see 'Anodic bonding'). So Pyrex glass 7740 which has the comparative thermal expansion to silicon was used. Pyrex 7740 wafers consist of 81% SiO_2, 13% B_2O_3, 4% Na_2O, 2% Al_2O_3. The other reason Pyrex 7740 glass is used in anodic bonding to silicon is due to the high content of mobile sodium ions. The large amounts of non-silicon-dioxide "impurities" give it noticeably different etching characteristics. Specifically, it etches slower than soda lime in 5:1 buffered HF. According to [3], the etch rate for Pyrex 7740 wafer in 5:1 BHF is 43 nm/min. A more aggressive solution of 5:1 Nitric Acid and HF is used to accelerate the etching procedure. Table 5.3 shows the etch conditions where the photoresist mask maintains integrity in the Pyrex 7740 etching solution. It can be seen with photoresist mask, Pyrex glass 7740 cannot be etched deeper than 0.5μm with NH_4F before the mask has been damaged. Using aluminum mask, it can be etched with HF and Nitric Acid (more aggressive than NH_4F) easily.

	Solution	Time mins	Temp.	Photoresist Mask	Under microscope	profilometer	
						Max μm	Average μm
Soda Lime	1:5 ($HF:NH_4F$)	3'40	room	Good	clear margin		
Soda Lime	1:5 ($HF:NH_4F$)	4'30	room	Good	clear margin		
Soda Lime	1:5 ($HF:NH_4F$)	3'40	room	Good	clear margin	5.7	3
Pyrex 7740	1:5 ($HF:NH_4F$)	3'40	room	Good	clear margin		
Pyrex 7740	1:5 ($HF:NH_4F$)	4'30	room	Good	clear margin		
Pyrex 7740	1:5 ($HF:NH_4F$)	6'	room	Good	clear margin	0.46	0.25
Pyrex 7740	1:5 ($HF:NH_4F$)	12'	room	damaged	damaged		
Pyrex 7740	1:2 ($HF:NH_4F$)	4'	room	damaged	damaged		
Hard Mask				Aluminum Mask			
Pyrex 7740	1:5 ($HF:HNO_3$)	3'40	room	Good	clear margin	0.7	0.5
Pyrex 7740	1:5 ($HF:HNO_3$)	4'30	room	Good	some margin damaged	3.2	3
Pyrex 7740	1:3 ($HF:HNO_3$)	2'30	room	Gone	some margin damaged	0.2	0.2
Pyrex 7740	1:4 ($HF:HNO_3$)	3'00	room	Gone	clear margin	2.2	2

Table 5.3 Etching condition when Soda Lime and 7740 are used

The biggest change in our procedure from soda lime to Pyrex 7740 is to use a hard mask instead of photoresist mask. This change was required because photoresist

1813 cannot stay in a 5:1 Nitric Acid and HF mixture for over 30 seconds. Since the etching depth we need to reach is 4 μm, the etch time is 120 seconds which exceeds the photoresist integrity time. Therefore, during deep wet etching of Pyrex 7740 wafer, an aluminum is used as the hard mask.

5.3.5 Aluminum, Gold, and Titanium Etching

Aluminum etch is performed during glass wafer steps (4) and (7). Gold and titanium are etched during step (12) (See chapter 3). Basically aluminum is used as hard mask during our procedure. The gold and titanium layer is used as a seed layer for electroplating. A solution of 16:1:1:2 (H_3PO_4:HNO_3:Acetic acid:H_2O) is used for aluminum etching. 1:3 (HNO_3:HCl) and 1:1:20 (HF:H_2O_2:H_2O) is used for gold and titanium etching, respectively.

The etch rate for Al is 530 nm/min at 50°C but slower at room temperature. Since 200nm Al is deposited as hard mask, the etch process takes 23 seconds. However, when the etch is performed, 3 minutes at 50°C and 6 minutes at room temperature is required. The etch rate for Au is 680 nm/min and Ti is 1100 nm/min [6]. Because the seed layer is very thin, the etch process only takes seconds. Also photoresist 1813 cannot be etched by Aluminum etchant, so it can be used as masks for the Aluminum etch.

5.4 Rates Determination of Boron Doping

5.4.1 Introduction

Boron doping is a high temperature process that diffuses boron atoms into the silicon wafer. Boron atoms provide extra holes to the silicon substrate, which makes it more conductive. The boron doping of the silicon has two tasks in our procedure. The first task is forming a highly conducting layer in the silicon wafer which serves as one of the capacitor plates. The second and more important task is the use of the doped region as an etch stop to realize the diaphragm thickness of 4 μm. In our case, an n-type wafer was doped with boron. An etch stop for KOH etching is achieved in regions with a boron concentration larger than 10^{20} atoms/cm^{-3}.

5.4.2 Silicon Doping Process

Boron Nitride p-type source wafers, BN-1250, from Saint-Gobain Ceramics are used for the boron doping process. They are composed of 40% BN and 60% SiO_2. Several important steps will be specified next.

1) Source Preparation: Since BN-1250 are BN and SiO_2 compositions, it is necessary to remove some of the SiO_2 with an HF dip followed by a DI-H_2O rinse. This etches some of the SiO_2 away to expose the boron nitride for oxidation. After the surface etch step, a water rinse is done to remove any residual HF. Routine re-etching may be necessary as the exposed BN is consumed. This is after use of 10 to 15 times.

2) Push in and Recovery: During the recovery step, source boats stacked with

BN-1250 wafers and silicon wafers are pushed into a diffusion tube. The tube is then allowed to establish ambient equilibrium. This step is generally performed in an ambient of 50% N_2 and 50% O_2 at 750°C-850°C. The N_2/O_2 ambient during the recovery step grows a thin layer of SiO_2 in the mask window regions. This thin layer of SiO_2 masks B_2O_3 diffusion during the push in cycle, thus minimizing or eliminating the sheet resistivity gradients due to the first wafer in being the last wafer out.

3) Soak: During the soak step, the dopant glass which is uniformly coating the silicon wafers undergoes a reduction reaction in the ambient which results in the formation of a thin insoluble layer of silicon-boride, Si-B, at the silicon surface. The Si-B layer serves to trap crystal damage at the silicon/ SiB interface through a strong gettering action. In essence, the function of the soak step is to control damage while obtaining the targeted sheet resistivity (see Figure 5.2).

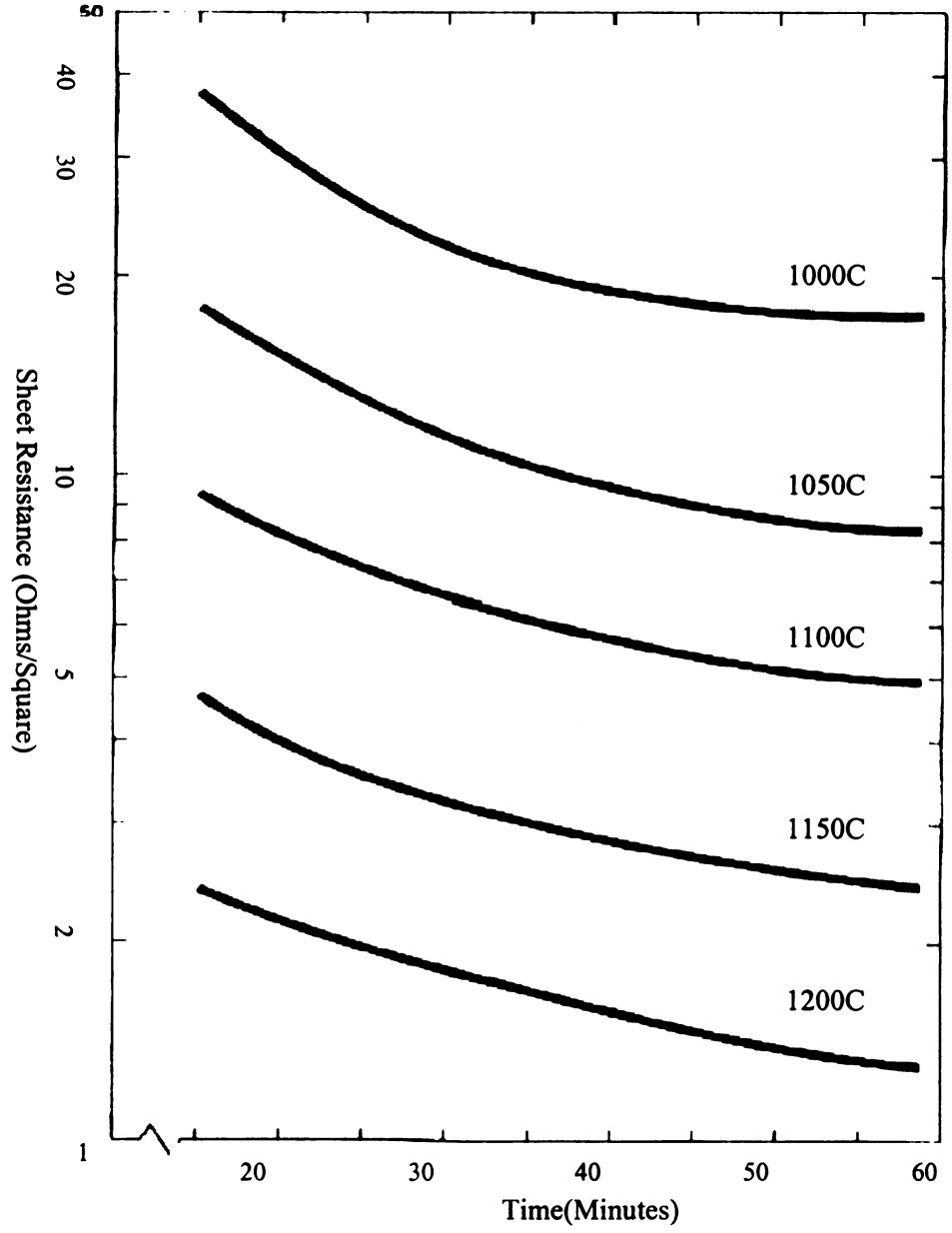

Figure 5.2 Sheet Resistance vs. Deposition Time and Temperature for BN-1250 [10]

4) Deglaze: After the Si wafers are unloaded from the furnace, the excess un-reacted dopant glass is removed by 10 parts Di-H_2O to 3 Parts HF for 2 minutes at room temperature.

5) Low Temperature Oxidation (LTO): The function of the LTO step is to oxidize

the Si-B layer and a thin layer of Si below it. Oxidizing this thin Si layer will immobilize most of the crystal defects in the oxide. A steam or O_2 ambient is typically used to cause the rapid oxidation of the Si-B layer and its silicon interface region before harmful propagation of the defects into the silicon can occur. This allows the subsequent drive cycle to be damage free.

5.4.3 Diffusion Calculation

The Silicon doping processes used in this investigation occurs by thermal diffusion. Thermal diffusion we use is described by Fick's Laws. The solution to the diffusion equation is:

$$N(x,t) = N_0 \cdot erfc\left(\sqrt{\frac{x^2}{4D_1t_1}}\right) \qquad [5.5]$$

Here N_0 is surface concentration which is maintained at $4*10^{20}cm^{-3}$. D_1 is the diffusion coefficient. Both are functions of the temperature. erfc() is the complementary error function. N(x,t) is thus the boron concentration at a certain time, t, and depth, x.

Low Temperature Oxidation (LTO) process is a further diffusion of boron atoms into the silicon lattice. Therefore, a higher concentration can be reached at larger depths in comparison to the soak step. The LTO concentration follows a Gaussian distribution and is given by: [11]

$$N(x,t) = \frac{2N_0\sqrt{D_1t_1}}{\pi\sqrt{D_2t_2}} \cdot \exp\left(\frac{-x^2}{4D_2t_2}\right) \qquad [5.6]$$

Index 1 is for soak step while index 2 is for LTO. Calculation of t_1 at 1200°C and t_2 at 800°C is listed below.

$$D = D_0 \exp(-E_A / kT) \qquad [5.7]$$

T_1 = 1200+273.15 = 1473.15K, T_2 = 800+273.15 = 1073.15K, D_0 = 166.3cm^2/s, E_A = 4.08eV, k = 8.62*10^{-5}eV/K [11]

Using [5.7], an approximation of D_1 can be found as 1.85*10^{-12}cm^2/s. D_2 is 1.16*10^{-17}cm^2/s.

Then N_0 = 4*10^{20} cm^3, x = 4*10^{-4} cm (4 μm), N = 10^{16} cm^3 put into [5.5]

$$10^{16} = 4*10^{20} \cdot erfc\left(\sqrt{\frac{x^2}{4D_1 t_1}}\right) \qquad [5.8]$$

Get t_1 = 2.40*10^3 seconds = 40 minutes. Put t_1 into [5.6]

$$t_1 = \frac{1}{4} \cdot N^2 \cdot \frac{\pi^2}{N_0^{\,2} \cdot \exp\left(-\frac{1}{4} \cdot \frac{x^2}{D_2 t_2}\right)^2} \cdot t_2 \cdot \frac{D_2}{D_1} \qquad [5.9]$$

Using Matlab, get t_2 = 7.79*10^2 seconds = 13 minutes.

5.5 Electroplating Rates

5.5.1 Introduction

Electroplating is the deposition of a metallic coating onto an object by putting a negative charge onto the object and immersing it into a solution which contains a salt of the metal to be deposited. The metallic ions of the salt carry a positive charge and are

attracted to the part. When they reach it, the negatively charged part provides the electrons to "reduce" the positively charged ions to metallic form.

5.5.2 Solution

After deposition of a seed layer by ebeam evaporation, electroplating is done to increase the gold thickness from 100 nm to 4 μm. Gold is a precious metal, which means that it will not oxidize in air, so its electrical conductivity stays uniform over long periods of time. It is ideally suited for electroplating applications. A gold electroplating solution with 99.99% purity is used in our experiment.

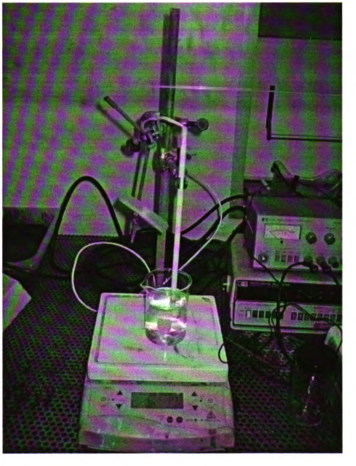

Figure 5.3 Setup of electroplating

Electroplating is a galvanic process, where the desired layer material is ionized in liquid and the coating sample is connected to a power supply as a cathode. Platinum coated titanium probe is used as the anode due to its noble metal properties and its high countervoltage. Most commonly used gold plating solutions contain cyanide, which is very toxic and thus hard to handle. That is why we decided to use a cyanide free gold solution which is limited to a gold concentration of about 8 g/l. The solution contains a $Na_3Au(SO_3)_2$ complex with the ability to dissociate and deliver Au^+ ions. Once dissociated the Au^+ ions are attracted to the negative substrate leading to the formation of a gold layer. This process is controlled by time and current density. In order to get enough dissociated gold atoms the liquid was heated to about 66°C. A magnetic stirrer was used to improve the uniformity of the deposited layer. The best results were reached at 100 rpm. The layer thickness is calculable by the following equation: [12]

$$d = \frac{I}{A} \cdot \frac{t \cdot m_A}{z \cdot e \cdot \rho} \qquad [5.10]$$

where I/A is the current density, m_A the mass per atom, z the valency (1 for Au), e the elementary charge and ρ the density. However, the calculation is just an approximation because the density of the coated layer is different to the bulk material density. To establish the optimum processing condition, several experiments were done with different current densities. Then the optical microscope and SEM were used to measure the electroplating rate and result. An optimum result was 120 μA when there is fifteen sensors in the solution. The electroplating time is 1 hour to get 4 μm thick gold windings.

References:

1. Nathan Cheung, EE143 Lecture #5, U.C. Berkeley

2. W. R. Runyan and K. E. Bean, "Semiconductor Integrated Circuit Processing Technology", Addison-Wesley Publishing Company, 1990

3. Kirt R. Williams, Kishan Gupta, and Matthew Wasilik, "Etch Rates for Micromachining Processing—Part II", Journal of Microelectromechanical Systems, Vol. 12, No. 6, December 2003

4. R. Booth, "Polycrystalline Diamond Thin-Film Fabry-Perot Optical Resonators on Silicon", Doctor dissertation, Dept. ECE, MSU, 2003

5. "Wet-Chemical Etching and Cleaning of Silicon", Virginia Semiconductor, Inc., January 2003

6. K. Sato et al., "Characterization of orientation-dependent ethcing properties of single-crystal silicon: effects of KOH concetration", *Sensors and Actuators A 64* (1988) 87-93

7. R. Hull, "Properties of Crystalline Silicon", INSPEC, London, 1999

8. H. Seidel, L. Cseprege, A. Heuberger, H. Baumgarel "J. Electrochem. Soc.", (USA) vol. 137 (1990) p. 3626-32

9. D.L. Kendall, "Annu. Rev. Mater. Sci", (USA) vol.9 (1979) p.373

10. J.B. Price "Semiconductor Silicon", Eds. 1973

11. D. K. Reinhard, "Introduction To Integrated Circuit Engineering", Houghton Mifflin Company, Boston Graphics, 1987

12. A. Kenneth Graham, "Electroplating Engineering Handbook", Van Nostrand Reinhold Company, 1971

Chapter 6

Process Flow

6.1 Introduction

This chapter describes the experimental aspect of this research, including the detailed manufacturing steps. The goal of this chapter is to convey an understanding of the methods used to create the samples in this research. In the actual fabrication of the devices, many individual devices or components will be made from a single wafer, and the entire wafer will be fabricated at once. Hundreds of devices can be completed simultaneously.

The fabrication of the device involves a series of steps. As outlined in Chapter 3, the whole fabrication procedure can be divided into three parts. The first part is fabrication of the silicon wafer, the second part is fabrication of the glass wafer, and the last part is the assembling and deep back etching of the silicon. So at the beginning of this chapter, a complete detailed fabrication "recipe" for the eye pressure sensor is presented. Then each step such as the oxidation, photolithography steps and the gold/titanium deposition, boron doping etc. will be documented. This chapter documents the detailed process times and procedure based on the experiments described in the previous chapters. The measurements during every step of the procedure will be introduced in the next

chapter; they will help make the process more controllable and repeatable.

6.2 Complete Fabrication Procedure

6.2.1 Silicon Wafer Part

1) Substrate cleaning (Total estimated process duration: 2 hours)

- Put sample in acetone ultrasonic bath for 30 minutes
- After rinse with De-Ionized(DI) water, put it in methanol ultrasonic bath for 30 minutes
- Rinse with DI water again and evaporate isopropanol on the wafer to relieve water from substrate
- !!!Special wafer cleaning procedure when the wafer is hard to clean with the steps above: Solution: 10:2:1 (H_2O:H_2O_2:NH_4OH), leave the wafer in 100ml H_2O, 20 ml H_2O_2, and 10 ml NH_4OH for 10 minutes
- Put sample in oven at 200°C for 30 minutes

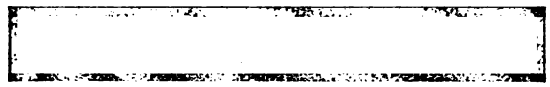

Figure 6.1 After Silicon Part Step1: Substrate cleaning

2) Thermal oxidation of the wafer to get oxide thickness of 1.4μm (Total estimated process duration: 13 hours)

- Use the thermal oxidation furnace for following steps
- Load wafer to glass boat and push it in the center of furnace
- Turn on the cooling water
- Switch on the fan on the furnace backside
- Switch on the heating pad and adjust to 40 in order to keep the water temperature steady
- Turn on oxygen
- Turn lever above the flow meter to the left (left: oxygen will go through heated water first, then to the chamber; right: oxygen go directly to the chamber)
- Set oxygen flow to 50 steel ball
- Switch on element and power on furnace front side
- Adjust to 800(400+800); a gage temperature of about 980°C will be reached
- Hold temperature for 12.5 hours
- Cool down and unload wafer
- Turn gas off and switch the power, the element and the heat pad off
- Let fan and cooling water run until gage shows less than 100°C

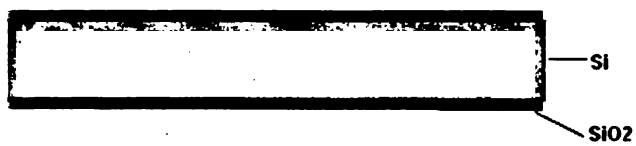

Figure 6.2 After Silicon Part Step2: Thermal oxidation

3) Photoresist spinning on both sides of wafer and lithographic step (Total estimated process duration: 1 hour and 30 minutes)

- Spin HMDS (Hexamethyldisilazane Adhesion Promoter) and Shipley 1813 (Positive photoresist with 1.3 μm thick) at 3000 rpm for 30 seconds on one side of substrate
- Put sample in oven for 10 minutes at 70°C
- Take wafer out and place it carefully upside down on spinner
- Spin HMDS and Shipley 1813 on the wafer
- Put sample back in oven for 30 minutes at 70°C
- Mask aligner process of the upper side: use the wafer positioning mask to position the mask 1 and the wafer.
- Exposure 2 times for 60 seconds (together 120 seconds)
- Develop in MF319 for 2 minutes
- Rinse under DI water and dry with nitrogen gun
- Put wafer in oven for 40 minutes at 130C, this is called "hard bake". afterwards cool down slowly

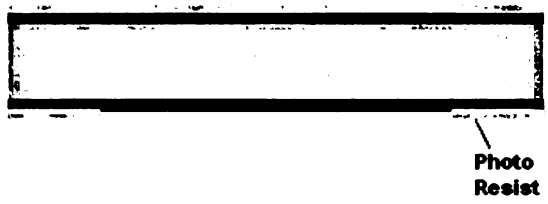

Figure 6.3 After Silicon Part Step3: lithographic step

4) SiO_2 etching (Total estimated process duration: 10 minutes)

- Solution: 1:5(HF:NH_4F), 10ml HF and 50 ml NH_4F
- Etch wafer for 10 minutes at room temperature
- Rinse under DI water

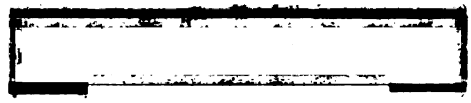

Figure 6.4 After Silicon Part Step4: SiO2 etching

5) Photoresist removal (Total estimated process duration: 5 minutes)

- Put wafer in acetone UltraSonic bath for 5 min.
- Rinse under DI water

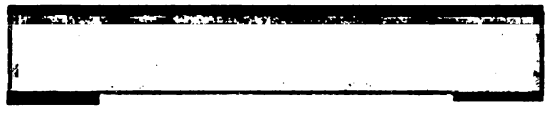

Figure 6.5 After Silicon Part Step5: Photoresist removal

6) Slow Silicon etching to form cavity (Total estimated process duration: 45 minutes)

- Solution: 40 grams KOH pellets (85%) with 60 ml DI water as etchant
- Put beaker on hot plate and adjust probe temperature to 100°C
- Set probe temperature to 62°C after 53 – 55 °C is reached
- Put sample in the etchant for exact 5 minutes after 62°C is reached
- Rinse wafer under DI water thoroughly
- Dry with nitrogen gun and put it in oven for 30 minutes at 200°C

- Cool down slowly

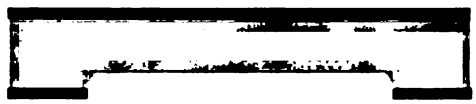

Figure 6.6 After Silicon Part Step6: Slow Silicon etching to form cavity

7) Photoresist spinning (Total estimated process duration: 30 minutes)

- Spin HMDS and Shipley 1813 at 3000 rpm for 30 seconds on the non-etched substrate side
- Bake in oven for 30 minutes at 130°C
- Cool down slowly

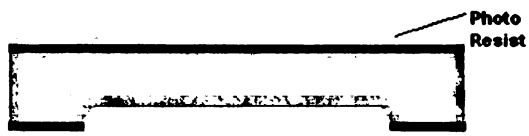

Figure 6.7 After Silicon Part Step7: Photoresist spinning

8) SiO_2 removal (Total estimated process duration: 10 minutes)

- Etch wafer for 10 minutes in 1:5 (HF:NH_4F), 10 ml HF and 50 ml NH_4F solution at room temperature
- Rinse under DI water

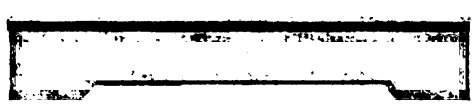

Figure 6.8 After Silicon Part Step8: SiO_2 etching

9) Photoresist removal and cleaning (Total estimated process duration: 30 minutes)

- Put wafer in acetone ultrasonic bath for 5 minutes
- Rinse under DI water
- Put wafer in new acetone ultrasonic bath for 20 minutes
- Rinse with DI water and evaporate isopropanol to relieve water from substrate
- Dry with nitrogen gun and put it in oven for 30 minutes at 200°C
- Cool down slowly

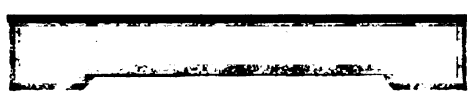

Figure 6.9 After Silicon Part Step9: Photoresist removal and cleaning

10) Boron Nitride (BN) wafer activation (Total estimated process duration: 3 hours and 30 minutes)

- !!! This step is only necessary when the B_2O_3 glass is completely gone, this means after use of 10-15 times!!!
- Etch in 3:2 DI-H_2O:HF(49%) for 2 minutes at room temperature
- Rinse with DI water for 2 minutes and dry with nitrogen gun
- Load BN wafer to the boat and put in the thermal diffusion furnace center
- Dry wafer there for 2 hours with 100% nitrogen – 60 steel ball at 400°C (adjust wheel to 0)

- Oxidize wafer for 30 minutes at 1000°C (adjust wheel to 545) and 100% oxygen – 60 steel ball
- Stabilize wafer for 30 minutes at 1200°C (wheel to 725) and 100% nitrogen – 60 steel ball
- Cool down slowly

11) Boron doping (Total estimated process duration: 2 hours and 30 minutes)

- Use the thermal diffusion furnace
- Same turn-on procedure like above (thermal oxidation) except the heat pad
- Set temperature to 850°C (adjust wheel to 375)
- Set nitrogen to 100% - steel ball 60
- Load the silicon wafer with the etched side face to face to the BN wafer in the boat when 800°C is reached
- Let boat stay in the furnace neck for 2 minutes to equilibrate
- Push in the boat very slowly in the furnace center, not faster than 10 cm/min
- Let wafer stabilize there for 10 minutes at 850°C
- During the recovery step, set nitrogen to 50% - steel ball 30, set oxygen to 50% - steel ball 30
- Let wafer stay there for 5 minutes at 850°C
- Then set nitrogen to 130 black ball and turn off oxygen
- Rise temperature to 1200°C (wheel at 740)
- Hold temperature for diffusion time – 60 minutes (soak step)

- Decrease temperature to 800°C (wheel at 325)
- Pull out boat slowly, not faster than 10 cm/min
- Let boat stay in the furnace neck for 2 minutes
- Take boat out and allow wafers to cool down, put BN wafer back in box
- Keep oven and nitrogen running
- Prepare 30ml HF(45%) and 100ml DI water
- Drop this solution with a pipette on the doped surface for 2 minutes and make sure that no liquid contacts the wafer backside (Deglaze step)
- Rinse thoroughly with DI water and dry with nitrogen gun
- Put wafer in the oven for 5 minutes at 200°C
- Place wafer back in boat (without BN wafer)
- Let boat stay in furnace neck for 2 minutes
- Push boat into the furnace slowly, not faster than 10 cm/min
- Once in the center, turn off nitrogen and turn on oxygen at 60 steel ball
- Let wafer oxidize for 20 min. at 800°C (called Low Temperature Oxidation, LTO)
- Afterwards turn off oxygen and turn on nitrogen at 60 steel ball
- Pull out slowly like above
- Let boat stay in furnace neck for 2 minutes
- Turn off nitrogen
- Turn off furnace system like described above (by thermal oxidation)
- Allow wafer to cool down

- If the surface still has some fog(boron glass), perform the same etch procedure like described above (with the pipette), the surface should be clean now (no fog)
- rinse with DI water and dry with nitrogen gun
- put it in oven for 30 minutes at 200°C

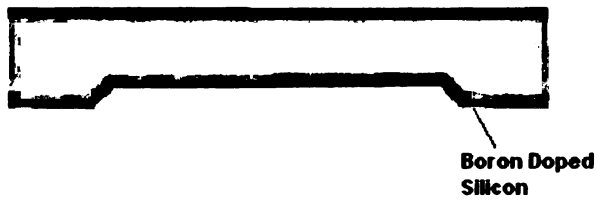

Figure 6.10 After Silicon Part Step11: Boron doping

12) Photoresist spinning and lithographic step on top side (Total estimated process duration: 2 hours and 15 minutes)

- Put wafer in acetone ultrasonic bath for 20 minutes, rinse with DI water
- Perform isopropanol evaporation to remove the water
- Put in oven for 30 minutes at 200°C
- Cool down slowly
- Spin HMDS and Shipley 1813 at 3000 rpm for 30 seconds on substrate
- Put sample in oven for 30 minutes at 70°C
- Mask aligner process (use mask 2); use the wafer positioning mask and the marks to position mask 2 and the wafer
- Exposure 2 times for 60 seconds each (together 120 seconds)
- Develop in MF319 for 2 minutes

- Rinse under DI water and dry with nitrogen gun
- Put wafer in oven for 30 minutes at 130°C (hard bake), afterwards cool down slowly

Figure 6.11 After Silicon Part Step12: Photoresist spinning and lithographic step on top side

13) SiO_2 etching (Total estimated process duration: 15 minutes)

- Solution: 1:5 (HF:NH_4F), 10 ml HF and 50 ml NH_4F
- Etch wafer for 10 minutes at room temperature
- Rinse under DI water

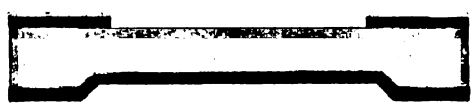

Figure 6.12 After Silicon Part Step13: SiO_2 etching

14) Photoresist removal and cleaning (Total estimated process duration: 30 minutes)

- Put wafer in acetone ultrasonic bath for 5 minutes
- Rinse under DI water
- Put wafer in new acetone ultrasonic bath for 20 minutes
- Rinse with DI water and evaporate isopropanol to relieve water from substrate

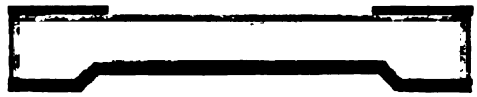

Figure 6.13 After Silicon Part Step14: Photoresist removal and cleaning

6.2.2 Glass Wafer Part

1) Substrate cleaning (Total estimated process duration: 2 hours)

- Put sample in acetone ultrasonic bath for 30 minutes
- After rinse with De-Ionized(DI) water put it in methanol ultrasonic bath for 30 minutes
- Rinse with DI water again and evaporate isopropanol to relieve water from substrate
- Put sample in oven at 200°C for 30 minutes

Figure 6.14 After Glass Part Step1: Substrate cleaning

2) Aluminum deposition (Total estimated process duration: 7 hours)

- Turn on nitrogen and chiller on the PVD system
- Load the Pyrex glass wafer into the chamber and load aluminum crucible to the crucible holder

- Switch to "start" on the main power and verify all 4 red LED's are on for the water flow indicators (below system in cabinet)
- Open the "Roughing" valve and SRS ion gauge controller
- Pump down to $5*10^{-6}$ Torr. It will take at least 5 hours
- Deposit Aluminum to one side of the wafer for about 200nm, deposition speed is no more than 1.0 Å/sec
- Afterwards store the wafer to the oven at 100°C

Figure 6.15 After Glass Part Step2: Aluminum deposition

3) Lithography step: defining coil, capacitor plate and electrical contacts (Total estimated process duration: 1 hour and 30 minutes)

- Spin HMDS and Shipley 1813 at 3000 rpm for 30 seconds on one side of substrate
- Put sample in oven for 30 minutes at 70°C (soft bake), afterwards cool down slowly
- Mask aligner process: use the wafer positioning mask and the marks to position mask 3 and the wafer
- Exposure for 70 seconds
- Develop in MF319 for 1 minute

- Rinse under DI water and dry with nitrogen gun
- Put wafer in oven for 30 minutes at 130°C (hard bake)
- Afterwards cool down slowly
- Observe coils under the microscope and check the dimensions

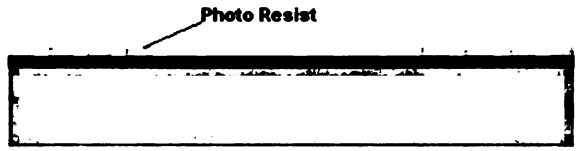

Figure 6.16 After Glass Part Step3: Lithography step: defining coil, capacitor plate and electrical contacts

4) Aluminum etching (Total estimated process duration: 10 minutes)

- Solution: 16:1:1:2 (H_3PO_4:HNO_3:Acetic acid:H_2O), 80 ml H_3PO_4, 5 ml HNO_3, 5 ml Acetic acid, and 10 ml H_2O
- Etch time 6 minutes at room temperature
- Rinse with DI water quickly after etching for at least 2 minutes
- Dry with nitrogen gun
- Observe the result under the microscope and check the pattern

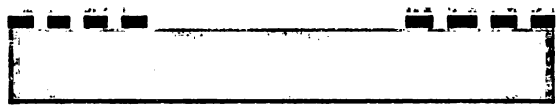

Figure 6.17 After Glass Part Step4: Aluminum etching

5) Pyrex glass etching (with depth of 2 microns) (Total estimated process duration: 40 minutes)

- Solution: 1:5 (HF:HNO_3), 10 ml H_3PO_4 and 50 ml HNO_3
- To get a constant etch depth, take a new solution for every wafer
- Etch time 4 minutes and 30 seconds
- Rinse with DI water quickly after etching for at least 2 minutes
- Dry by nitrogen gun
- Observe the result under the microscope and check the pattern, if there are bubbles etc. in the trench, rinse under DI and etch again
- Put sample in oven for 30 minutes at 100°C

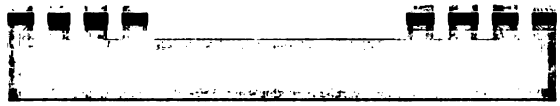

Figure 6.18 After Glass Part Step5: Pyrex glass etching

6) Photoresist removal (Total estimated process duration: 30 minutes)

- Put wafer in acetone ultrasonic bath for 30 minutes
- Rinse under DI water

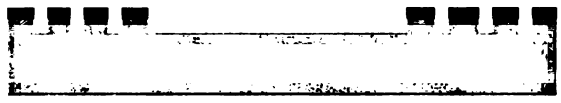

Figure 6.19 After Glass Part Step6: Photoresist removal

7) Aluminum removal (Total estimated process duration: 40 minutes)

- Solution: 16:1:1:2 (H_3PO_4:HNO_3:Acetic acid:H_2O), 80 ml H_3PO_4, 5 ml HNO_3, 5 ml Acetic acid, and 10 ml H_2O
- Put beaker on the hotplate, heat to 50°C, etch for 3 minutes
- Rinse with DI water and dry with nitrogen gun
- Put in the oven for 30 minutes at 100°C

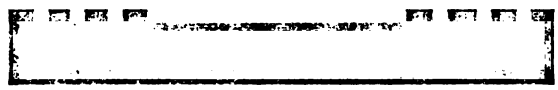

Figure 6.20 After Glass Part Step7: Aluminum removal

8) PVD process to coat Titanium and Gold seed layer (Total estimated process duration: 6 hours)

- Turn on nitrogen and chiller
- Load the Pyrex glass wafer to the chamber and load aluminum crucible to the crucible holder
- Switch to "start" on the main power and verify all 4 red LED's are on for the water flow indicators (below system in cabinet)
- Open the "Roughing" valve and SRS ion gauge controller
- Pump down to $5*10^{-6}$ Torr and it will take at least 5 hours
- Deposit 5nm Titanium on the wafer, and then deposit 50nm Gold for a seed layer. Deposition speed should be no more than 0.5 Å/sec
- Afterwards store the wafer in the oven at 100°C

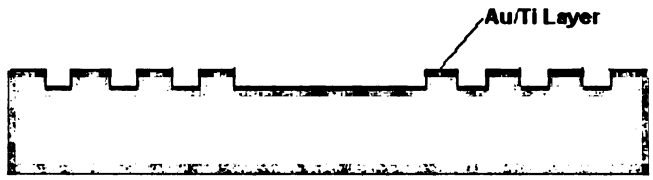

Figure 6.21 After Glass Part Step8: PVD process to coat Titanium and Gold seed layer

9) Lithography step (including mask alignment) (Total estimated process duration: 1 hour and 30 minutes)

- Spin HMDS and Shipley 1813 at 3000 rpm for 30 seconds on one side of substrate
- Put sample in over for 30 minutes at 70°C (soft bake), afterwards cool down slowly
- Mask aligner process; use the wafer positioning mask and the mark to position mask 3 and the wafer.
- Use the mask aligner microscope to align the pattern on the mask with the pattern on the glass wafer
- Exposure for 70 seconds
- Develop in MF319 for 1 minute
- Rinse under DI water and dry with nitrogen gun
- Put wafer in oven for 30 minutes at 130°C (hard bake)
- Afterwards cool down slowly
- Observe coils under the microscope and check the dimensions

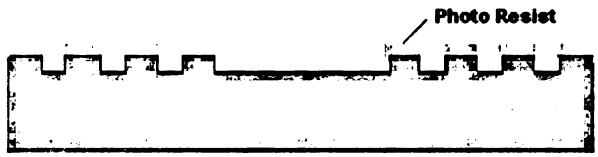

Figure 6.22 After Glass Part Step9: Lithography step (including mask alignment)

10) Electroplating: deposition of 4 μm gold (Total estimated process duration: 1 hour)

- Set up the plating system
- Make sure that approximately 200 ml plating solution is in the beaker
- Set stirrer to 100 rpm
- First pre-set probe temperature to 200°C
- After 54 - 55°C is reached, set probe temperature to 66°C
- After 66°C is reached, we can start the plating process
- Put the glass wafer down to the solution
- Set the current to be 120 μA
- Plating time can be decided as following: 15 sensors (in the solution) for 60 minutes
- Afterwards rinse wafer with DI water

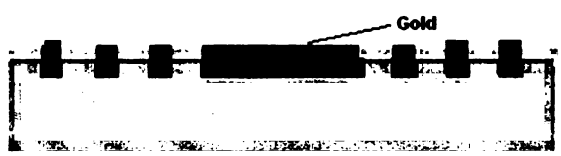

Figure 6.23 After Glass Part Step10: Electroplating: deposition of 4 microns gold(Au)

11) Removal of Photoresist with acetone (Total estimated process duration: 10 minutes)

- Put sample in acetone ultrasonic bath for 10 minutes
- Rinse under DI water

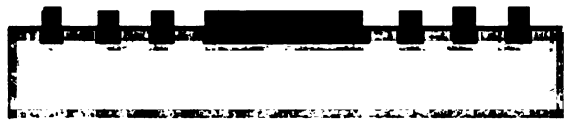

Figure 6.24 After Glass Part Step11: Removal of Photoresist with acetone

12) Thin Au/Ti layer removal (Total estimated process duration: 10 minutes)

- Solution for etching gold: 1:3 (HNO_3:HCl), 30 ml HNO_3, and 10 ml HCl
- Solution for etching titanium: 1:1:20 (HF:H_2O_2:H_2O), 5 ml HF, 5 ml H_2O_2 and 100 ml H_2O
- Etch time: 20 seconds at room temperature until the clear glass wafer comes up
- Rinse with DI water quickly after etching
- Dry by nitrogen gun
- Observe the result under the microscope and check the pattern

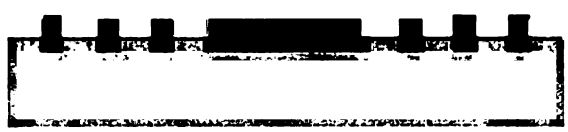

Figure 6.25 After Glass Part Step12: Thin Au/Ti layer removal

6.2.3 Assembling Part

1) Cleaning procedure (Piranha) (Total estimated process duration: 40 minutes)

- Put both wafers (Pyrex glass wafer and silicon wafer prepared before) together with 30 ml H_2SO_4 in a glass beaker
- Add 10 ml H_2O_2 in the beaker carefully (starts to bubble) for 5 minutes
- Rinse wafers under DI water and dry with nitrogen gun
- Put wafers in oven for 30 minutes at 130°C

2) Anodic bonding (Total estimated process duration: 30 minutes)

- Set up bonding system in following sequence (listing is from the bottom): heat plate, glass plate, aluminum plate with connector, silicon wafer, glass wafer (alignment need to be operated before bonding)
- Connect aluminum plate to positive pole on power supply (screw)
- Connect the probes to the negative pole and let them touch the glass surface
- Adjust temperature to 550°C
- Turn on the power supply when 400°C is reached
- Start with 100V, increase the voltage about 100V every 10 sec. until 1000V is reached
- Turn OFF power supply IMMEDIATELLY if a current starts to flow (large than 5mA)
- Black area (bonded area) starts to spread around the probes
- Once bonded, turn down voltage slowly and switch off power supply

- Remove bonded wafer from set-up and put it in oven which is preheated to 250°C and let it cool down slowly

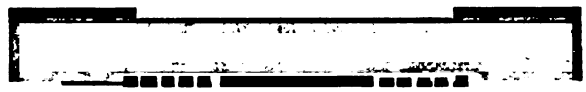

Figure 6.26 After Assembling Part Step2: Anodic bonding

3) Back silicon etching (Total estimated process duration: 5 hours)

- Put 150ml DI water and 80g KOH (85%) in a glass beaker
- Heat glass beaker until a liquid temperature of 100°C is reached
- Put bonded wafer into liquid
- Try to hold liquid temperature constant
- Etch until doped region is reached (this will reduce etch speed which means less bubbles will come out, it will take 4 hours)

Figure 6.27 After Assembling Part Step3: Back silicon etching

4) Separation

- One wafer combination houses 243 sensors
- Separate the sensors with diamond wire saw

- Use wax to fix the wafer on the rubber substrate
- adjust the wire to the desired direction
- keep the water running to avoid the wire too hot
- One cut will usually cost 20 minutes

6.3 Conclusion

All processes in this chapter have been developed and implemented. Complete glass wafers and silicon wafers have already been manufactured. In the following chapter, the results of the experiment will be presented.

Chapter 7

Experiment Results

7.1 Introduction

In this chapter, we will discuss the results of the experiment to achieve the design of the eye pressure sensor. Every primary procedure will be introduced with data, including thickness of the oxidation layer and boron doping layer, etching results, resisitivity of the boron doping region, electroplating results and SEM results.

7.2 Results of thermal oxidation

7.2.1 Calculation and Experiment Result

For a target oxide thickness of approximately 1.3 μm, The Linear and Parabolic Growth Laws indicate approximately 8 hours of wet oxidation at 1000°C, or 80 hours of dry oxidation at 1200°C. Apparently we should choose wet oxidation to save some time. However, the ideal, 100% wet oxidation considered in the model can be difficult to achieve in the laboratory without considerable effort. Recognizing that 8 hours would be insufficient, the wafers had been oxidized for 12.5 hours at 980°C. The weight of the wafer was measured before and after the oxidation. The weight gained during the oxidation is used to estimate the resulting oxide thickness.

The method to calculate the oxide thickness is via weight gain measurement. First we need two assumptions: 1) The total number of silicon atoms in the wafer does not

change, and 2) all of the weight gain comes from oxygen atoms bonding with the silicon in the wafer to form a SiO_2 layer. [1] So

$$w_{OX} = \left(1 + \frac{28.09}{2 \times 16.0}\right) \times w_g \qquad [7.1]$$

Here w_{OX} is the weight of the SiO_2 on the wafer. w_g is related to the measured weight gain. The atomic mass of silicon and oxygen is 28.09 and 16.0. Additionally, it is assumed that the wafer is a perfect 3-inch diameter circle and that oxide growth on the edges can be neglected. This means that the thickness of the oxide layer on one side of the wafer, t_{OX}, can be determined by using the density of SiO_2, ρ_{OX}, and w_{OX}.

$$t_{OX} = \frac{w_{OX}}{2 \times \rho_{OX} \times \pi \times r^2} \qquad [7.2]$$

Thermal SiO_2 is amorphous. The weight density ρ_{OX} is 2.2 grams per cubic centimeter and r is 3.81 cm. So

$$t_{OX} = 0.00936 \times w_g \qquad [7.3]$$

where the unit of t_{OX} is in cm and w_g is in grams. Expressed in units of μm and grams,

$$t_{OX} = 936 \times w_g \qquad [7.4]$$

A common rule of thumb is that the thickness of silicon consumed by the oxidation is 44% of the thickness of the final resulting oxide layer. As the SiO_2 layer is grown on a silicon surface, a certain thickness of the silicon is lost. This means that after the oxidation, the thickness of the wafer t_w is approximately:

$$t_w = 300 - 2 \times 0.44 \times t_{OX} = 300 - 823.68 \times w_g \qquad [7.5]$$

where the factor of two accounts for the fact the silicon is consumed from both surfaces. Again the unit for t_w is μm and w_g is in grams, and a starting thickness for the wafer of 300μm is considered.

Table 7.1 is the oxide thickness results after several experiments. Figure 7.1 compares the results with the Linear and Parabolic Growth Laws. (see Chapter 5.2)

time hrs	adjusted T °C	gage T °C	thickness μm	result
13	900	750	0.75	very uniform SiO_2 layer
12	1000	790	0.78	very uniform SiO_2 layer
13	1000	790	0.8	very uniform SiO_2 layer
10	1200	980	1.0	very uniform SiO_2 layer
11	1200	980	1.2	very uniform SiO_2 layer
12.5	1200	980	1.3	very uniform SiO_2 layer
12.5	1200	980	1.3	very uniform SiO_2 layer

Table 7.1 Thermal Oxide thickness

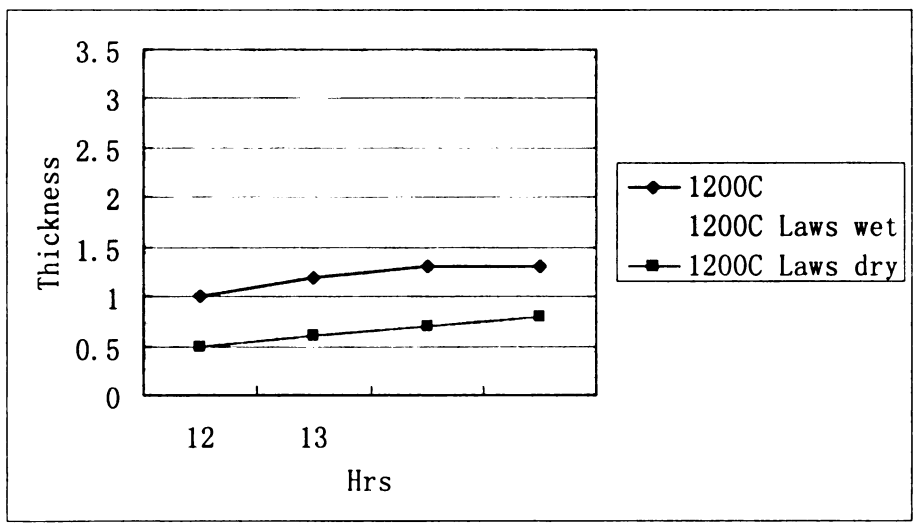

Figure 7.1 Thermal Oxide Thicknesses vs. Time

7.2.2 Discussion

During this thermal oxidation process, a Thermco diffusion furnace was used. A heated bubbler containing De-ionized (DI) water was used to provide steam for the oxidation. Grade 5.0 oxygen (meaning "five-nines" or 99.999% pure) was pumped through the bubbler and into the furnace at an approximate rate of 200 standard cubic centimeters per minutes (sccm).

The oxide thickness is calculated by weight gain measurement. Weight gain measurements showed that these growth conditions resulted in an oxide layer approximately 1.3 μm thick. This is slightly less than the target oxide thickness, but was found adequate for masking purposes. As shown in Figure 7.2, the oxide was grown on the silicon wafer.

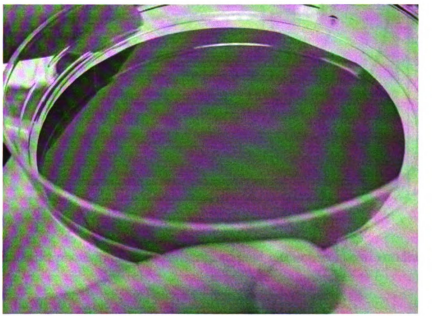

Figure 7.2 Silicon Wafer after Thermal Oxidation

7.3 Discussion of Lithography Step

Sample alignment becomes an issue during our experiment. When we are doing the glass fabrication process step 9 (See Chapter 6), first we use the wafer positioning mask to position the mask #3 and the wafer. Then the microscope is used to align the pattern on the mask with the pattern on the glass wafer. Misalignment can make the whole wafer useless. As Figure 7.3 and 7.4 shows, the electroplated gold will move off the trench, so the coil windings will not be continuous.

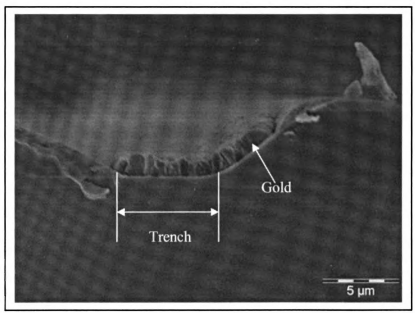

Figure 7.3 SEM photograph of the misaligned gold electroplated coil windings (Cross Section)

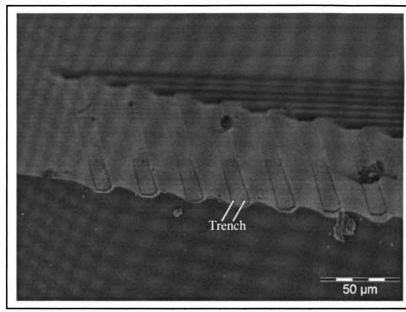

Figure 7.4 SEM photograph of the misaligned gold electroplated coil windings, the electroplated gold has moved off the trench (Top Surface)

Several efforts have been made to improve the accuracy of alignment. First we tried to get the patterns on the sample and the mask approximately parallel (Two position marks are on the wafer). Then we move to an alignment spot close to an edge and move the microscope to an alignment spot near the opposite edge. Correct approximately half of the misalignment with the angular adjustment and the remaining misalignment with the X or Y micrometer. Several iterations of this method gave a good alignment. Figure 7.5 and 7.6 shows the good alignment.

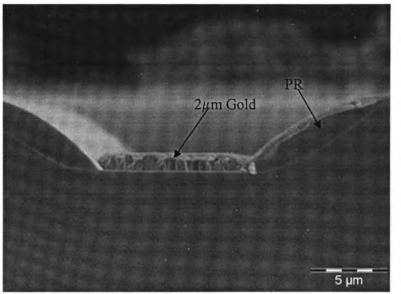

Figure 7.5 SEM photograph of the aligned gold electroplated coil windings (Cross Section)

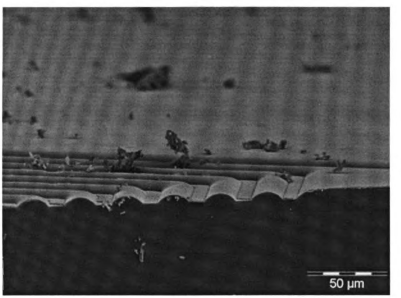

Figure 7.6 SEM photograph of the aligned gold electroplated coil windings (Top Surface)

7.4 Results of Etching Step

7.4.1 Results of Silicon Etching

Several microscope pictures show here that the roughness of the silicon etching region is changing versus time for the deep silicon back etch. The surface becomes smoother when the etching time increases. Finally it will get smooth once the boron doped layer is reached.

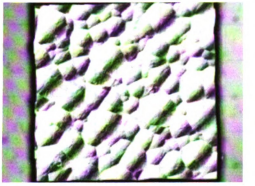

Figure 7.7 Silicon etching for 15 minutes with 40% KOH 95°C

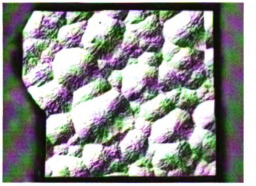

Figure 7.8 Silicon etching for 30 minutes with 40% KOH 95°C

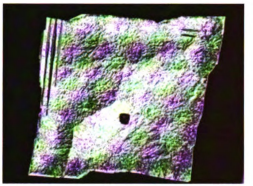

Figure 7.9 Silicon etching for 116 minutes with 40% KOH 95°C

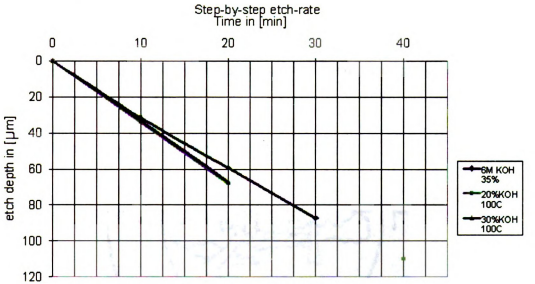

Figure 7.10 Step by step etching rate

Figure 7.10 shows the etching rate from our experiment. This is for the deep back etching. For this etch step the temperature is set to 100°C, and the etch rate is around 3.0 μm/min.

For silicon wafer step4 (see chapter 6), we use 40% KOH and a temperature of 62°C. The slow etch rate is about 0.3 μm/min. Figure 7.11 shows the SEM picture of the pattern of silicon etching region.

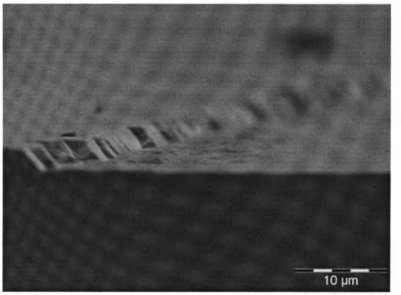

Figure 7.11 SEM picture of the pattern of silicon etching region

7.4.2 Results of Pyrex Glass Etching

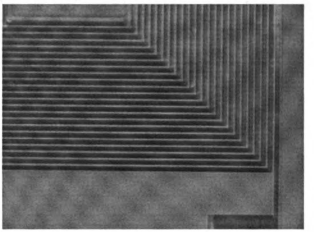

Figure 7.12 Top view of the Pyrex glass after etching

For the Pyrex glass etch an etching depth of 4μm is wanted, which takes about 120 seconds (see chapter 5.3). During deep wet etching of the Pyrex 7740 wafer, Aluminum is used as the hard mask. Figure 7.12 gives us a top view of the Pyrex glass after etching.

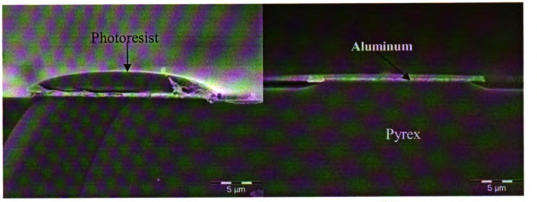

(a) (b)

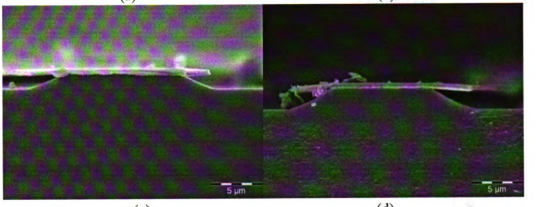

(c) (d)

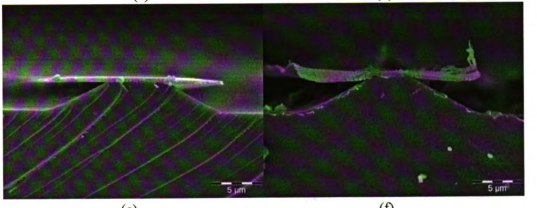

(e) (f)

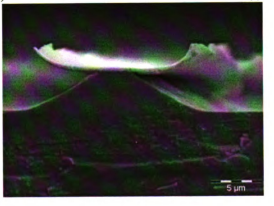

(g)

Figure 7.13 SEM photos showing the cross-section of etched cavities

Figure 7.13 SEM photos show the cross-section of etched recesses in the Pyrex 7740 glass wafers at 7 different depths. (a) before Pyrex etching, (b) after 20 seconds etching, (c) after 40 seconds etching, (d) after 60 seconds etching, (e) after 80 seconds etching, (f) after 100 seconds etching, and (g) after 120 seconds etching. Figure 7.14 shows Pyrex 7740 etch depth vs. time. Figure 7.15 shows the etching rate.

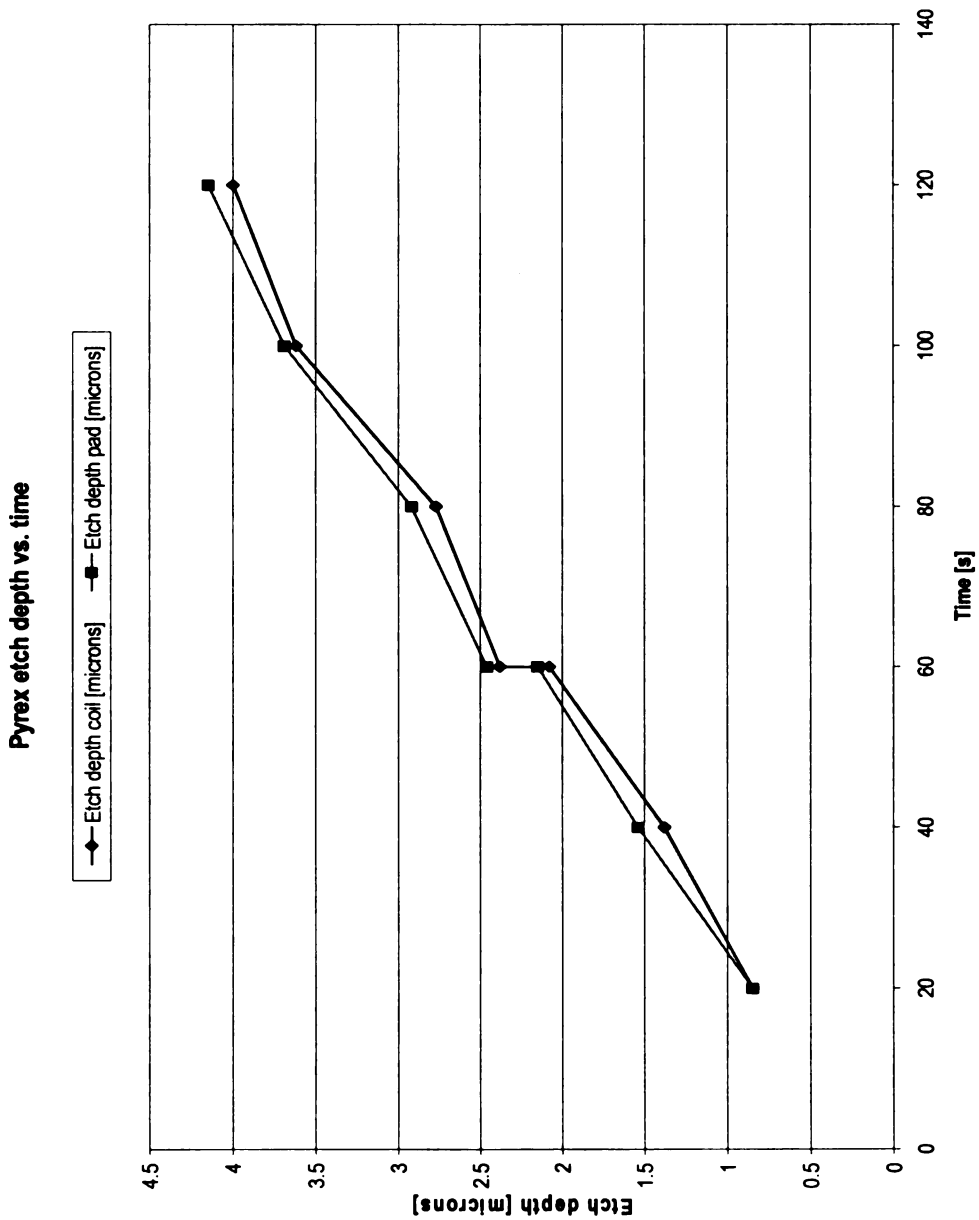

Figure 7.14 Pyrex 7740 etch depth vs. time.

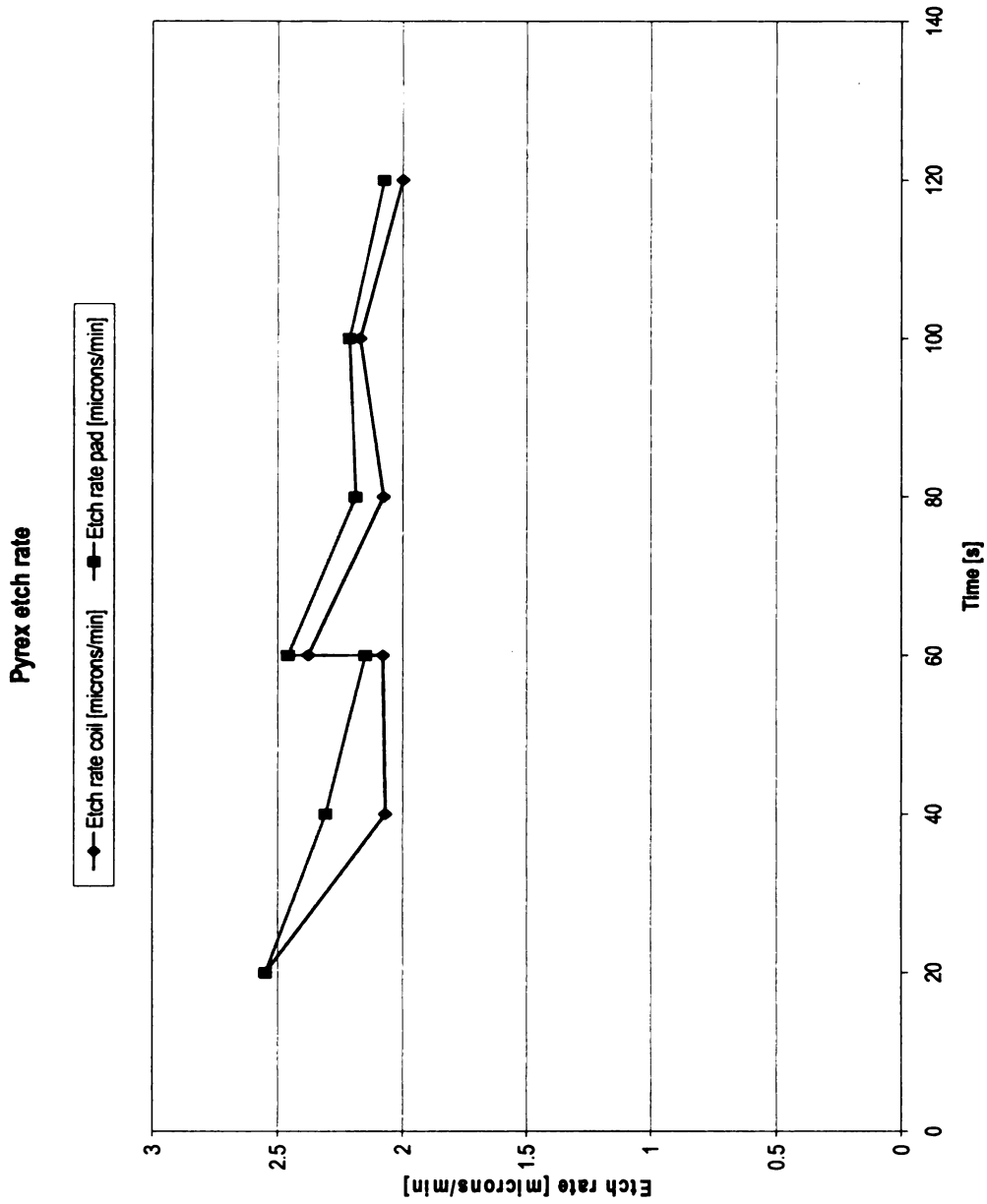

Figure 7.15 Pyrex 7740 etching rate

7.5 Experiment Results of Boron Doping

Based on the calculation in chapter 5.4.3, the soak time used in experiment in minutes is 40 at 1200°C and LTO time is 13 at 800°C. There was some difference between the calculated values and the values used in the lab because the actual reading of internal temperature of furnace differed from the calculated values.

Every boron doped wafer is measured for its sheet resistivity by a four probe measurement. Figure 7.16 shows sheet resistivity vs. time when the furnace temperature is 1200°C.

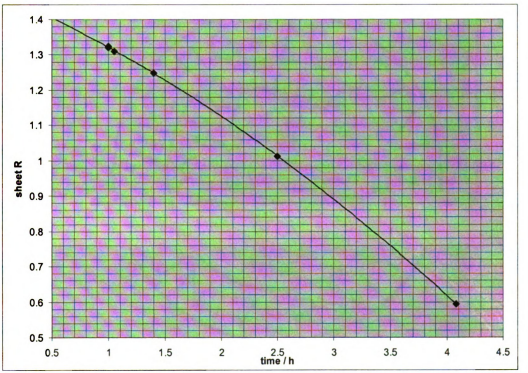

Figure 7.16 sheet resistivity vs. soak time when the furnace temperature is 1200°C

7.6 Experiment Results of Electroplating

Four microscopic photos after electroplating are shown in Figure 7.17 where the experiment set-up is unchanged but the electroplating time is different. The photographs show that the width of the gold windings is varying as the electroplating time changes.

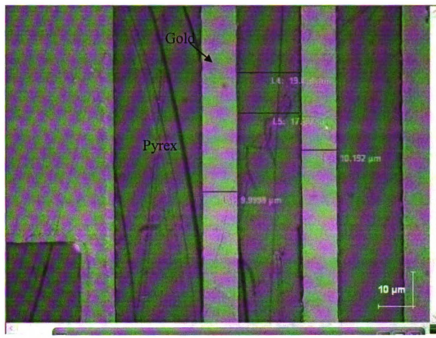

(a)

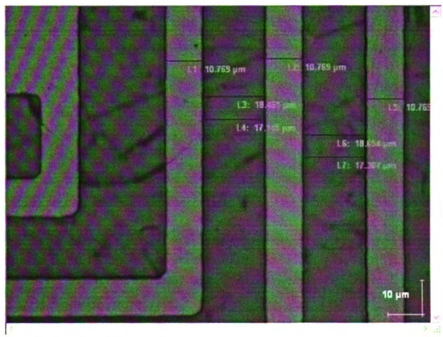

(b)

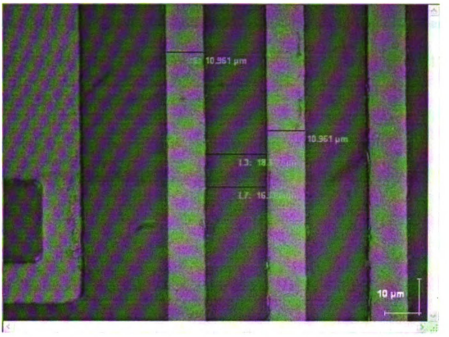

(c)

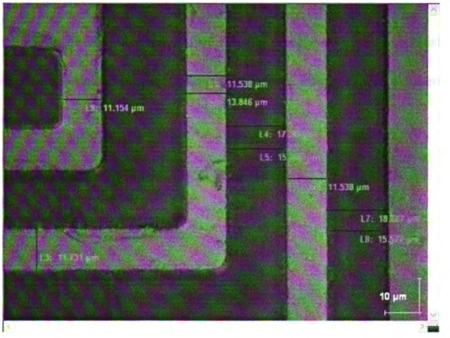

(d)

Figure 7.17 Microscopic Photos after Electroplating

For the electroplating step twelve sensors are done in the solution at a time. The current used is 180 μA. The plating times for the SEM picture in Figure 7.17 are: (a) 15 minutes (b) 20 minutes (c) 30 minutes (d) 45 minutes. We can see in Figure 7.17 that the width of the gold coil is increasing versus time.

7.7 Resonant Frequency Measurement

7.7.1 Measurement Circuit

There are two circuits used in the setup. The primary circuit consists of a signal generator, resistor and inductor. The resistor voltage is displayed on the oscilloscope as the output signal. The secondary circuit, which is the eye pressure sensor, consists of an inductor and a capacitor. This circuit resonates at a given frequency due to the energy storing abilities of its components.

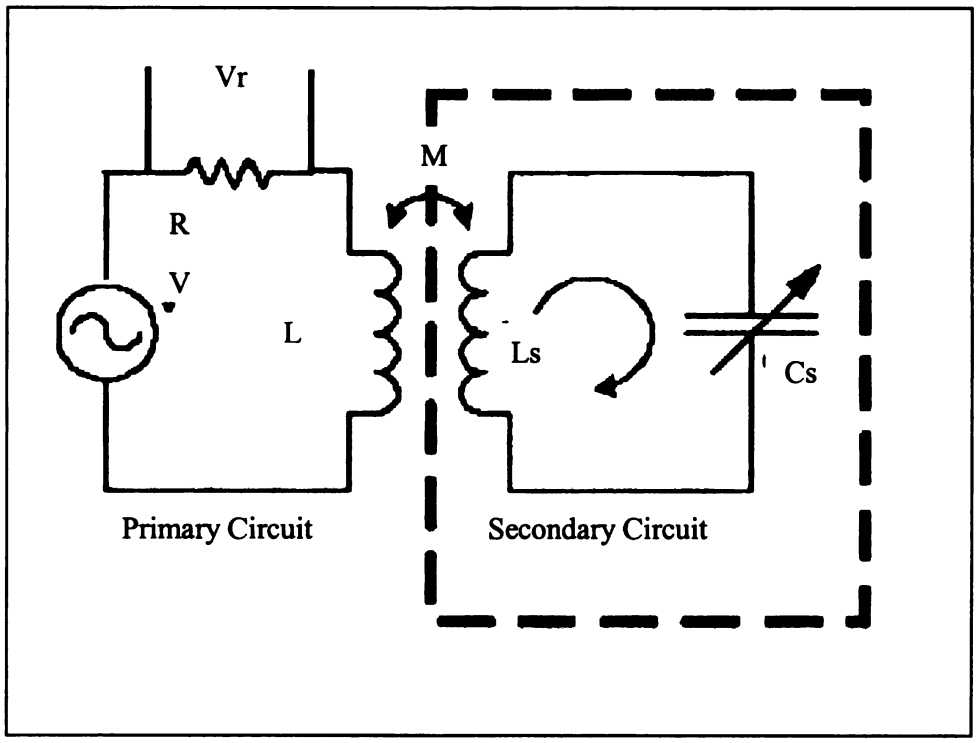

Figure 7.18 Measurement Circuit

7.7.2 Resonant Frequency Simulation

A systematic way is developed to simulate for the resonant frequency of the eye pressure sensor. The following Pspice file proved useful for simulation:

For eye pressure sensor resonance frequency simulation:

```
Vin 1 0 AC 1.0V                ;Voltage generator

R1 1 2 160                     ;Primary circuit resistor

L1 2 0 0.259U                  ;Primary circuit inductor


L2 3 0 0.3U                    ;Secondary circuit inductor;
```

```
C1 4 0 8.2P          ;Secondary circuit capacitor;
R2 3 4 6             ;Resistance due to wires;

K12 L1 L2 0.1        ;Creates mutual inductance between L1 and L2
                     ;Larger K increases the width and height of
                     ;spike: 0.03<K<0.4

C2 1 2 8P            ;Represents capacitance due to 10:1 probe
C3 2 0 1P            ;Represents capacitance due to coil windings

.AC DEC 2000 1Hz 200MegHz
.PROBE
.END
```

Figure 7.19 shows the simulation result. Inflection point yields the true resonant frequency of secondary circuit. The resonant frequency of the circuit can be estimated at about 101 MHz in Figure 7.19.

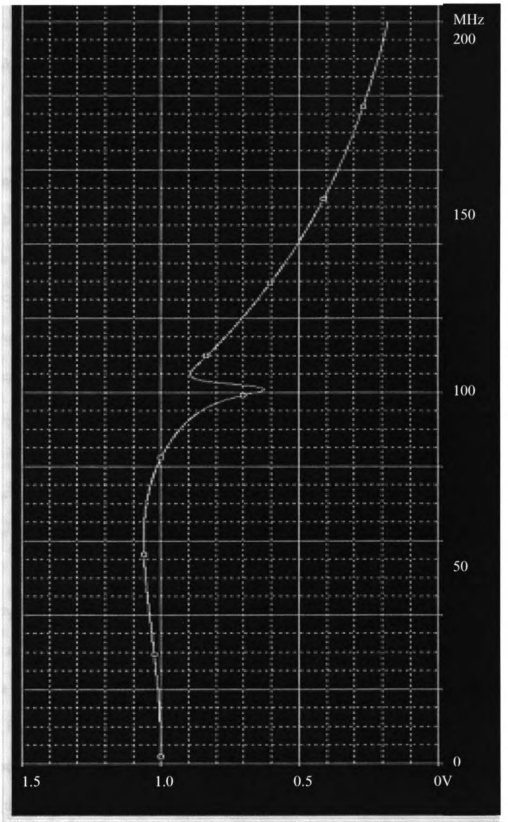

Figure 7.19 Simulation of the resonance frequency of the secondary circuit

7.7.3 Resonant Frequency Measurement

A completely fabricated intraocular pressure sensor that gives a working response as shown in Figure 7.19 has not been achieved yet. However, a partially fabricated sensor has been tested and found to exhibit the LC resonance. This device had the pyrex portion of the sensor completely fabricated and the silicon portion partially fabricated. Specifically, the silicon part was boron doped but not back etched. To insure a contact between the silicon and pyrex parts, a thin (20nm) Gold layer was deposited and patterned on the silicon boron doped side before the bonding of the parts. Using a test circuit as shown in Figure 7.18, the spectral response as shown is Figure 7.20 was obtained. For Figure 7.20 the external resistor R shown in Figure 7.18 was not included, rather the circuit relied on the internal resistance of the voltage supply which is estimated to be 50 ohms.

As can be seen in Figure 7.20, the frequency generator does not output a constant voltage when the frequency is changed, so the input voltage to the circuit is not constant. The resonant frequency of the secondary IOP sensor circuit is about 300MHz. Figure 7.20 shows us the peak to peak value on the resistor voltage vs. frequency of the external coil itself (f2) and the voltage when the external coil is moved close to the pressure sensor (f1). The difference can be seen clearly in Figure 7.21, which shows the resonance frequency of fabricated sensor is around 300MHz.

Also a PSpice result is simulated to compare with resonance frequency of the fabricated IOP sensor. The capacitance of the secondary pressure sensor circuit has been changed from 8.2pF to 1pF and resistance from 6 Ω to 20 Ω. The reason to decrease the capacitance is the separation between the silicon wafer and the pyrex wafer of the test fabricated sensor is larger than the design value. This means the capacitor is smaller than the design value. For the resistance, although a thin Gold layer was deposited to insure a contact between the silicon and pyrex parts, a larger resistance (20 Ω) still needs to be considered because of the sheet resistance of the boron doped layer. From Figure 7.22, a LC resonance frequency moves to 300MHz and because of the resistance, the frequency band between the dip and peak becomes broader.

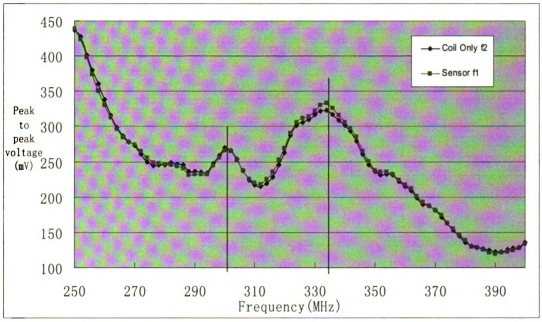

Figure 7.20 Resonance Frequency Measurement

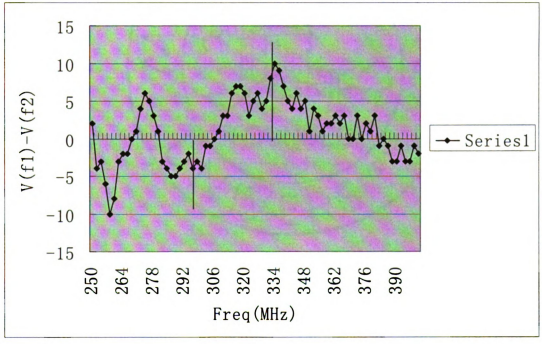

Figure 7.21 Resonance Frequency Measurement 2

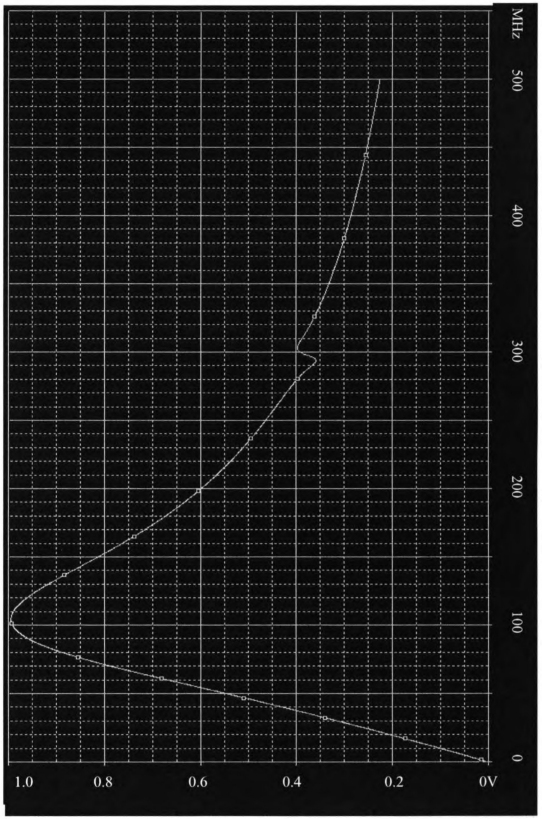

Figure 7.22 Simulation result of the fabricated IOP sensor

References:

1. Stephen A. Cambell, "The Science an Engineering of Microelectroic Fabrication", Oxford University Press, 1996

2. D. Reinhard, "Lecture Handout From EE 483 at Michigan State University", 2004

Chapter 8

Conclusions and Future Works

8.1 Conclusions

Glaucoma is one of the most dangerous diseases of the eye that exists today. High intraocular pressure (IOP) can be associated with much of the development and progression of glaucoma damage that occurs through time. The work in this thesis is to finish the fabrication of the actual device based on the design information obtained from the prototype device.

This thesis describes the manufacture and measurement for an implantable eye pressure sensor by using Micro Electrical Mechanical Systems (MEMS) technologies. The sensor will be implanted in the eyes of glaucoma patients to monitor intraocular pressure (IOP) on a continuous basis. This sensor is one of three components in a pressure measurement system. A complete detailed fabrication "recipe" for this eye pressure sensor has been presented in the thesis. A flow chart has been introduced to make every fabrication step clearly understood and visualized.

Now an implantable wireless capacitive pressure sensor has been designed and partially fabricated. The sensor has a simple structure and is obtained using a capacitive pressure sensor and a gold electroplated planar coil that forms an LC circuit. Applied pressure deflects the 4 μm-thin silicon diaphragm, changing the capacitance, and hence, the resonant frequency of the circuit. This change is sensed remotely with inductive coupling, eliminating the need for wire connection or implanted RF telemetry circuits to monitor the applied eye pressure. Fabricated devices measure 3.2x3.84 mm in size and houses 23 turns of a gold-electroplated coil. The sensor is designed to provide a resonant

frequency change around 100MHz for a pressure change in the range 0-50mmHg with respect to the eye liquid pressure.

The fabrication process of the sensor is based on the bulk silicon dissolved wafer process with some additional steps needed to integrate the on-chip electroplated coil with the pressure sensor. Fourteen manufacturing procedures are used including substrate cleaning, thermal oxidation, lithography step, etching for different kinds of material, boron doping, PVD deposition, electroplating, anodic bonding, separating, microscope measurement, scanning electron microscope, profilometer, four-point probe measurement, frequency scan measurement.

8.2 Recommendations for Future Research

Although eye pressure sensors have been fabricated, the complete frequency shift due to the external pressure change has not been seen. However, a partially fabricated sensor has been shown to give a resonance signal.

The resonant frequency of the partially completed sensor was higher than the design value. The reason is believed to be the difference between the actual capacitor plate separation and the design value. The separation of the capacitor plate is believed to be larger than the design value. This results in a lower capacitance value and a high resonance frequency. Another fabrication issue that remains is bonding the pyrex and silicon parts together with the appropriate pressure inside the sealed chamber. Currently the pressure inside the chamber is lower than the ambient pressure, since during the

sealing process with electrostatic glass to silicon anodic bonding, the structure is heated up to 500°C. When the device cools down, the air inside the sealed cavity produces a lower pressure and pulls the diaphragm closer to the fixed metal capacitor plate on the glass, increasing the zero pressure capacitance, hence, decreasing the resonant frequency of the sensor.

Another step will be designing and manufacturing of the processing unit and the database to get a complete usable pressure monitoring system. In combination with the processing unit, a calibration of each sensor will be necessary. The calibration will be performed in a precisely adjustable pressure chamber. Next the sensor will be implanted and the mode of operation tested. Once all tests are passed the sensor will monitor the eye pressure over longer periods and thereby help to cure eye troubles.

Various fabrication processes can also be improved. The thermal oxidation process has been used for our process. Michigan State University has a PECVD system which can deposit oxides and nitrides at lower deposition temperature, which in the future may be a better method of producing a masking layer for the silicon deep back etches due to both thermal budget considerations, as well as the possibility of an increased deposition rate. Additionally, plasma-assisted etching can be used to improve on some of the wet etching steps.